Proceedings of the 11th Brazilian Congress of Thermal Sciences and Engineering – ENCIT 2006
Braz. Soc. of Mechanical Sciences and Engineering – ABCM, Curitiba, Brazil, Dec. 5-8, 2006

Paper CIT06-0100

DISCRETE METHODS IN MICROHYDRODYNAMICS

P. C. Philippi[1], **L. O. E. dos Santos**[2], **C. E. Pico Ortiz**[3], **F. G. Wolf**[4],
L. A. Hegele Jr.[5], **R. Surmas**[6], **D. N. Siebert**[7]
Mechanical Engineering Department. Federal University of Santa Catarina.
88040-900 Florianópolis. SC. Brazil.
[1]`philippi@lmpt.ufsc.br`, [2]`emerich@lmpt.ufsc.br`, [3]`capico@lmpt.ufsc.br`, [4]`fgwolf@lmpt.ufsc.br`,
[5]`hegele@lmpt.ufsc.br`, [6]`surmas@lmpt.ufsc.br`, [7]`diogo@lmpt.ufsc.br`

Abstract. *In microhydrodynamics we are interested in solving flow problems in micro geometries, e.g., in porous media and micro heat pipes, where the fluid flow is frequently conditioned by surface forces and surface phenomena, such as in capillary flows, coalescence and surface break-off. In micro flows, the interaction forces at the fluid-fluid and fluid-solid interfaces play an important role in the description of the fluid flow. These forces are from a molecular origin and the translation of their effects to our macroscopic scales is a chief problem, considering that by its multiscale nature these phenomena do not, frequently, have a homogeneization scale. In this work, we present a mesoscopic method based on discrete models of the Boltzmann equation, which should provide the establishment of a conceptual bridge between the molecular and the macroscopic domains, in the study of microhydrodynamics.*

keywords: *Continuous Boltzmann equation, Lattice Boltzmann, discretization.*

1. Introduction

The purpose of this work is to discuss fluid mechanics problems when the spatial scale is very small and when the hydrodynamic balance equations cannot be closed by the use of simple rules. This is the case of micro flows, when the interaction forces at the fluid-fluid and fluid-solid interfaces play an important role in their description, Israelachvili, 1992.

Taking into account that these forces are from a molecular nature, the question to be placed here is how to translate the description of their effects from the molecular scale to our macroscopic scales, which are several order of magnitudes larger, considering that by its multiscale nature these phenomena, frequently, do not have a homogeneization scale.

In this work we present a mesoscopic method based on discrete models of the Boltzmann equation, which have been developed in very recent years, after 1990 and which should provide the establishment of a conceptual bridge between the molecular and the macroscopic domains.

Considering the molecular chaos hypothesis, Boltzmann considered a fluid as a mechanical system of particles with the purpose of demonstrating the *irreversibility*, a common attribute of classical thermodynamic systems but a *nonsense* in classical mechanics. Developed, in its origin, for monoatomic rarefied gases the Boltzmann equation has received several contributions in the course of the last 130 years by: i) the inclusion of finite volume effects in the Enskog's kinetic theory of dense gases, Enskog, 1921 ii) the consideration of the rotational, Lifshitz and Pitaevskii, 1999, and vibrational degrees of freedom, Wang Chang and Uhlenbeck, 1970, of the modelled particles, iii) the inclusion of electromagnetic effects in the study of plasmas, Tanenbaum, 1987. Recently, He and Doolen, 2002, proposed a split of the collision term in two parts for taking the long-range intermolecular attraction forces into account, in the kinetic description of liquids.

Lattice-Boltzmann models are discrete forms of the Boltzmann equation, when in addition to the discretization of time and of the physical space, the velocity space is also discretized, with the peculiarity that after each time step and following a local collision process the particles are propagated from each site to its next neighbours. The number of first neighbours to each site is related to the higher order of the kinetic moments that are to be described, Philippi *et al.*, 2006b.

In addition to the lattice-Boltzmann collision-propagation schemes (LBM) a number of alternative discrete velocity methods have been appearing in recent years based on finite differences, finite volumes and, more rarely, on finite elements numerical schemes, but the discussion of these methods is outside the scope of this work.

The lattice-Boltzmann equation (LBE) was introduced by McNamara and Zanetti, 1988, replacing the Boolean variables in the discrete collision-propagation equations by their *ensemble* averages. Higuera and Jimenez, 1989, proposed a linearization of the collision term derived from the Boolean models, recognizing that this full form was unnecessarily complex when the main purpose was to retrieve the hydrodynamic equations, with a very few relaxation parameters. Following this line of reasoning, Chen *et al.*, 1991, suggested replacing the collision term by a single relaxation-time term, followed by Qian *et al.*, 1992, and Chen *et al.*, 1992, who introduced a model based on the Bhatnagar-Gross and Krook (BGK) collision term (Bhatnagar *et al.*, 1954), retrieving the correct incompressible Navier-Stokes equations, with third-order non-physical terms in the local speed, u. In fact, the BGK collision term describes the relaxation of the distribution function to an equilibrium distribution, but in the above works, this discrete equilibrium distribution was settled by writting it as a *second-order polynomial expansion* in the particle-velocity $\vec{\xi}_i$, with parameters that were adjusted to retrieve the mass density, the local velocity and the momentum flux equilibrium moments, which are necessary conditions for satisfying the Navier-Stokes equations.

In trying to describe non-isothermal full compressible flows, thermal lattice-BGK schemes included higher order terms in the equilibrium distribution function (Alexander *et al.*, 1993, Chen *et al.*, 1994), requiring to increase the lattice dimensionality (Alexander *et al.*, 1993, McNamara and Alder, 1993, Chen *et al.*, 1994), i.e., the number of vectors in the finite and discrete velocity set $\left\{\vec{\xi}_i, i = 0, ..., b\right\}$, but the polynomial expansion form in the particle-velocity $\vec{\xi}_i$, with adustable parameters, was retained, the numerical simulations being peformed on, somewhat, empirically chosen lattices.

In thermal problems, BGK single relaxation time collision term restricts the models to a single Prandtl number. The full description of fluids and fluid flow requires multiple relaxation time models (MRT). A two-parameters model was introduced by He *et al.*, 1998, using two sets of distributions for the particles number density and the thermodynamic internal energy, coupled through a viscous dissipation term and proposed to be runned with a two-dimensional 9-velocities lattice. Full MRT models were firstly introduced in the LBE framework by d'Humières, 1992, d'Humières *et al.*, 2001, by modifying the collision step, considering it to be given by the relaxation to the equilibrium of a set of non-preserved kinetic moments.

Nevertheless, the presently known lattice-Boltzmann equation (LBE) has not been able to handle realistic thermal and fully compressible flow problems with satisfaction, since the simulation of the LBE is, frequently, hampered by numerical instabilities when the local velocity increases, Lallemand and Luo, 2003.

Considering the kinetic nature of the LBE, establishing a formal link between the LBE and the continuous Boltzmann equation, allowing the conceptual analysis of this discrete numerical scheme, could perhaps shed some light on this question. Indeed, there are several features that let the lattice Boltzmann regular-lattice based framework far away from the continuous Boltzmann equation, which would be desirable to be its conceptual support. These features include the particles model, the collision and long-range interaction models and the approach used for the time and the velocity space discretization.

With a few exceptions, in all the above works there is no formal link connecting the LBE to the continuous Boltzmann equation, although the main ideas were based on the kinetic theory fundamentals.

He and Luo, 1997, have directly derived the LBE from the continuous Boltzmann equation for some widely known lattices by the discretization of the velocity space, using the Gauss-Hermite and Gauss-Radau quadrature. Unhappily, excluding the above mentioned lattices, the discrete velocity sets obtained by this kind of quadrature do not generate space-filling lattices.

In a recent paper, Philippi *et al.*, 2006b, the velocity discretization problem was considered as a quadrature problem with prescribed abcissas, starting from the Boltzmann continuous equation, by requiring the discrete equilibrium distribution f_i^{eq} to have the same value of the continuous distribution f^{eq} when evaluated at a quadrature pole $\vec{c}_i$. In this manner, when the order of approximation N of a Hermite polynomial expansion to the MB equilibrium distribution is chosen, a set $\Psi_{\theta,(r_\theta)}$, $\theta = 0, ..., N$, of Hermite polynomials is established, and the infinite and enumerable basis of the Hilbert space $\mathcal{H} : c^D \rightarrow \mathcal{R}$, is replaced by a *finite* set of Hermite polynomial tensors, restricting the solutions to N^{th}-degree polynomials in the velocity $\vec{c}$. The quadrature problem was, then, considered as to select a regular lattice $\{\vec{c}_i\}$, in such a manner that functions $\Psi_{\theta,(r_\theta)}$ preserve the orthogonality with respect to the inner product in the discrete space. This was shown to be posible to be accomplished by assuring that the norm of *each one* of these functions $\Psi_{\theta,(r_\theta)}$ is retrieved, *exactly*, in the discrete space. The number b of the required lattice vectors is proportional to the order N of the polynomial approximation, $b = b(N)$ and, tt was,formally, shown that the lattice dimensionality is directly related to the order of approximation of the discrete equilibrium distribution, with respect to the full Maxwell-Boltzmann distribution and, consequently, to the highest order of the kinetic moments that are to be correctly described. In addition, it was shown that when the quadrature problem is solved, the 2θ-rank velocity tensors are isotropic in the discrete space, for $\theta = 1, ...N$. Similar results were, almost, simultaneously, obtained by Shan *et al.*, 2006, although using a different procedure.

An important practical result from Philippi *et al.*, 2006b, was to show that when the space-filling lattices are built taking lattice-vectors which are integer multiples of the D2Q9 velocity vectors, i.e., the DQ hierarchy, the 4^{th} kinetic moments, important in describing the flow of energy, *cannot be correctly described.*

Although the proposed method in Philippi *et al.*, 2006b leads to MRT collision models, the method has important differences with respect to D 'Humières moments method. In D'Humières moments method (d'Humières, 1992, d'Humières *et al.*, 2001), dispersion equations are used as constraints for the adjustable parameters related to the short wave-length, non-hydrodynamic, moments and numerical stability is assured by buffering these higher frequency moments. In Philippi *et al.* method (Philippi *et al.*, 2006b), non-physical lattice effects and numerical instability, in the description of higher-order hydrodynamic phenomena, can be only avoided by increasing the lattice dimensionality, required by the highest order of the kinetic moment to be preserved with the modelled LBE. The highest order of the kinetic moments possible to be correctly described with the LBE equation is limited by the number of lattice velocities, Philippi *et al.*, 2006b, and high-order kinetic moments are not correctly described when all the b-moments in a b-discrete velocities set are considered, as in the moments method. In fact, in currently produced works dealing with applications of the moments method, e.g. Lallemand and Luo, 2003, the main worry is *numerical stability* and *not* the description of non-isothermal, multicomponent or immiscible fluids flows, which, effectively, require additional relaxation parameters with respect to BGK models.

In this work, we present the lattice-Boltzmann framework, as a discrete method with its starting point at the Boltzmann continuous equation. Some important questions are discussed related with the suitability of this framework to solve non-isothermal, multiphase physical problems in microhydrodynamics.

In fact, although the LBM can be used for solving advection-diffusion problems, instead of the full set of macroscopic transport equations, which is the basis of classical CFD methods, some questions have been shown to be important to be answered considering the exciting possibility that is open in building the lattice-Boltzmann framework as a real bridge connecting the molecular to the macroscopic domain:

i) **Collision term**: When the particles are considered as material points without long-range interactions the modelled fluid follows an equation of state for ideal gases, $P = n_d kT$. In this manner the isothermal compressibility χ_T is high and the simulation of incompressible flows are subjected to compressibility effects, Surmas *et al.*, 2006. In LBM, these compressibility effects are usually avoided by working with small local velocities, but this restricts the simulations to low Reynolds numbers or requires to increase the number of lattice sites for high Reynolds number, increasing the computational costs and reducing LBM competitiveness with respect to conventional CFD methods. Enskog's collision term, Enskog, 1921, was derived considering the particles to be rigid spheres with a finite volume and the equation of state was derived as $P = n_d kT\ (1 + \rho b \chi)$ where b is related to the particle volume by unity mass and χ is a correction factor which can be written in terms of the mass density ρ, Chapman and Cowling, 1999. For liquids, the long-range attraction among particles was considered by He and Doolen, 2002, by splitting the collision term in two parts, the first part related to short-range interaction and the second one related to long-range interaction. After some simplifications, this second part was further written in terms of a mean interparticle potential and the equation of state was derived as a van-der-Waals *like* equation $P = n_d kT\ (1 + \rho b \chi) - a\rho^2$.

ii) **Collision model**. The collision term Ω is dependent on the distribution function itself and, indeed, the Boltzmann equation is a non-linear integro-differential equation that has been shown to be too difficult to be solved. Instead of the full collision term, a collision model is required leading to a non-linear partial differential equation, which can be numerically solved, Philippi *et al.*, 2006a.

iii) **Velocity discretization**. The distribution function depends on the particles velocity and this requires the discretization of the velocity space, in addition to the discretization of the physical space. Considering the required accuracy for a given discrete scheme, the problem is how to find the minimal number of discrete velocities for that given accuracy (Philippi *et al.*, 2006b, Philippi *et al.*, 2006c). In the present work, we deal with the lattice Boltzmann method (LBM) in space-filling lattices where, after each time-step, the particles are displaced from a given site to their next neighbors.

iv) **Boundary conditions**. In LBM, the boundary condition are reflection laws for the particle populations, since macroscopic variables such as velocity and temperature are not accessible as primitive variables. In certain cases, these boundary conditions can be related to velocity slips and temperature jumps that are difficult to overcome.

v) **Ideal mixtures**. Particles with different masses, at a given site, but with the same peculiar kinetic energy will be displaced to different points after a given time step, reaching intermediate positions between two contiguous sites and requiring the use of reallocation rules that, localy, preserve mass, momentum and energy. Interpolation schemes may be the source of numerical instability and alternative modelling strategies may show to be necessary, Ortiz *et al.*, 2006.

vi) **Non ideal mixtures and Immiscible fluids**. The electrostatic forces among the molecules produce the non-ideal behavior of fluids and fluid-mixtures and are at the origin of the phase separation process, when two immiscible fluids are put in contact, being responsible for the interfacial tension. These forces must be considered and correctly modelled in LBM.

Topics i), ii), iii), iv) and vi) are treated in some detail in present work.

2. Boltzmann equation as providing an alternative method for solving fluid mechanics problems

The Boltzmann equation can be derived from Liouville's equation, Cercignani, 1969, by supposing statistical independence for the 2-particle distribution function, in the limit when the number of particles N$\rightarrow\infty$, with a finite value of Nσ^2, σ being related to the particles diameter, $\sigma\rightarrow 0$. It reads

$$\partial_t f + \vec{\xi}.\nabla_r f + \vec{g}.\nabla_\xi f = \Omega, \tag{1}$$

where $\vec{r}$ is the position, $\vec{\xi}$ the particles translational velocity and $\vec{g}$ the acceleration due to the external forces.

The particles are considered as *material points without long-range interaction* and the collision term Ω in Eq. (1) must satisfy

$$\int \Omega m d\vec{\xi} = 0, \tag{2}$$

$$\int \Omega m\vec{\xi} d\vec{\xi} = 0, \tag{3}$$

$$\int \Omega \frac{1}{2} m\xi^2 d\vec{\xi} = 0, \tag{4}$$

due to the preservation of mass, momentum and kinetic translational energy in collisions.

In this manner when Eq. (1) is, respectively, multiplied by the mass, m, the momentum $m\vec{\xi}$ and the energy $\frac{1}{2}m\xi^2$, after some straightforward algebra, the following transport equations are obtained,

$$\partial_t\rho + \partial_\alpha\left(\rho u_\alpha\right) = 0, \tag{5}$$

$$\partial_t\left(\rho u_\alpha\right) + \partial_\alpha\left(\rho u_\alpha u_\beta + P\delta_{\alpha\beta} + \tau_{\alpha\beta}\right) = \rho g_\alpha, \tag{6}$$

$$\partial_t\left(\rho e\right) + \partial_\alpha\left(\rho e u_\alpha + q_\alpha\right) = -\tau_{\alpha\beta}\partial_\beta u_\alpha - P\partial_\alpha u_\alpha, \tag{7}$$

where ρe is the internal energy per unit volume, given, in this case, by

$$\rho e = \int f\frac{1}{2}m\left(\vec{\xi} - \vec{u}\right)^2 d\vec{\xi} \tag{8}$$

The equilibrium solution of the Boltzmann equation, Eq. (1) is the solution of,

$$\Omega = 0, \tag{9}$$

which can be shown to be a Maxwellian distribution, f^{eq}.

When this equilibrium distribution is required to satisfy

$$\int f^{eq} d\vec{\xi} = n_d, \tag{10}$$

$$\int f^{eq}\vec{\xi} d\vec{\xi} = n_d\vec{u}, \tag{11}$$

$$\int \frac{1}{2} m f^{eq}\left(\vec{\xi} - u\right)^2 d\vec{\xi} = \frac{D}{2} n_d kT, \tag{12}$$

where n_d is the local number density of the particles with mass m, $\vec{u}$ is the local velocity T, the local thermodynamic temperature, and D, the Euclidean dimension of the physical space, the Maxwell-Boltzmann distribution is retrieved,

$$f^{eq} = n_d \left(\frac{m}{2\pi kT} \right)^{D/2} e^{-\frac{(\vec{\xi}-\vec{u})^2}{\frac{2kT}{m}}}, \tag{13}$$

and the pressure P is related to the particles number density by the ideal gas law

$$P = n_d kT. \tag{14}$$

Further, a Chapman-Enskog analysis shows that in the continuous limit, $Kn \to 0$, the viscous stress tensor is given by

$$\tau_{\alpha\beta} = -\mu \left(\partial_\beta u_\alpha + \partial_\alpha u_\beta \right) + \kappa \delta_{\alpha\beta} \partial_\alpha u_\alpha, \tag{15}$$

and the heat flow vector by

$$\vec{q} = -\varkappa \nabla e. \tag{16}$$

In this manner, in the continuous limit, the Boltzmann equation, Eq. (1) gives the correct hydrodynamics for Newtonian fluids and can be used for solving advection-diffusion problems, instead of the full set of macroscopic transport equations, Eqs. (5-7), which is the basis of classical CFD methods.

Nevertheless, as a mesoscopic method we must consider the possibility that is open in building this framework not as an alternative numerical method, for solving the advection-diffusion equations, *but as a real bridge connecting the molecular to the macroscopic domain.*

In the next section we show some physical problems that require to downscale to be correctly understood.

3. Some physical problems in microhydrodynamics

Consider a capillary- rising problem, when a liquid raises inside a capillary tube against the gravity force, Figure 1.

Let $x_s(r,t)$ be the position of the liquid surface above the free liquid surface and consider the problem of finding the position x_s for any radius r at a time t. The question that we want to answer is how to find $x_s(r,t)$ from the solely information of the capillary tube diameter and the liquid wettability on the solid surface - given by the equilibrium contact angle, in static conditions, when a small liquid drop is put in contact with the surface of the capillary tube.

This problem has several simplified solutions, but all these solutions are based on an equilibrium contact angle (Lucas, 1918, Stange *et al.*, 2003, Washburn, 1921, Bosanquet, 1923) which is supposed to be constant during the rising process.

Furthermore, the exact solution of this problem via the hydrodynamic Eqs. (5-7) in the Stokes incompressible limit leads to a velocity singularity in the triple line, Dussan *et al.*, 1991. This singularity is easy to explain, since at the same time the triple line is responsible for the interface advancement, it must, also, satisfy an adherence condition of zero velocity at the solid surface.

In fact, the triple-line is not a *line*, but a transition region of some nanometers among the three phases (in this case: solid, liquid and gas) and where a liquid molecule is, simultaneously, subjected to the intermolecular forces from the adjacent liquid molecules - responsible for the liquid surface tension - and to the attractive forces from the solid surface -related to the work of adhesion between the liquid and the solid.

In this manner, the correct understanding of the capillary-rising problem requires, in principle, the knowledge of the fine physical structure of the triple-line and to solve a multi-scale problem, where the scales vary from some nanometers to several micrometers.

For understanding what happens in the triple line, some elementary knowledge of surface physical-chemistry is needed. Surface tension is responsible for keeping a liquid drop at the end of the overhanging branches of a three in rainning days, Figure 2. The intermolecular forces among the liquid molecules produce a tension state at the liquid surface. These forces can be considered as electrostatic forces that depend on the molecular shape, Figure 3. Asymmetric molecules such as the water molecule have a permanent dipole moment and attract themselves with polar (or Keesom) forces. The intermolecular forces among symmetric, non-polar, molecules,

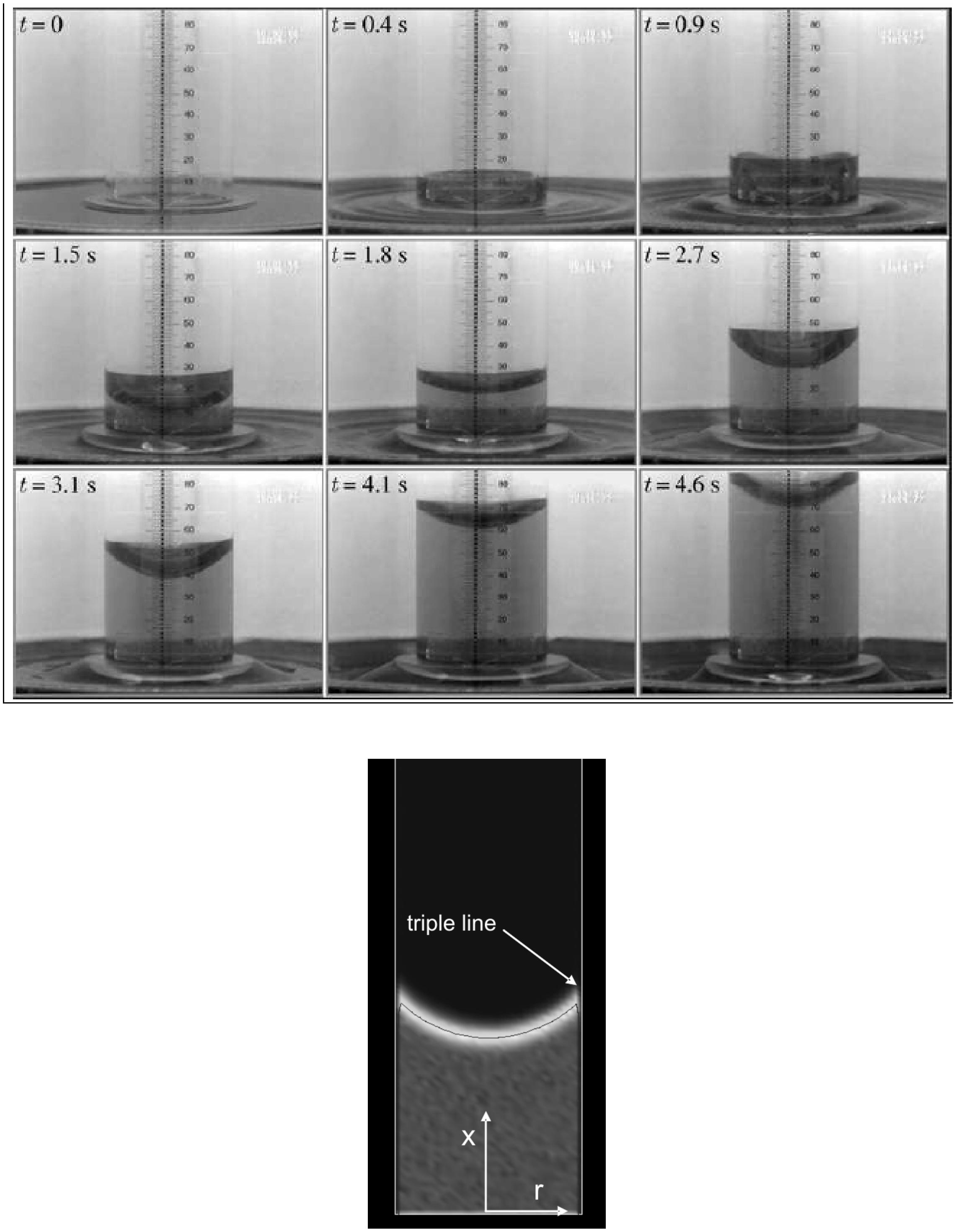

Figure 1: The triple line in capillary rising (from Stange *et al.*, 2003)

Figure 2: The surface tension counteracts the weight of a small liquid drop.

such as the hydrocarbon molecules, are due to the high frequency fluctuations of the geometrical center of theirs electronic clouds. These forces are called Bond or dispersive forces. When a polar molecule is near a non-polar molecule, the dipole moment of the polar molecule is subjected to high-frequency fluctuations due to the electrostatic Debye induction from the non-polar molecule and this interaction produces an attractive force which is of a dispersive nature. This cross force is frequently weaker when compared to the polar forces among the polar molecules and to the dispersive forces among identical non-polar molecules. In this manner, polar and non-polar liquids are, in general, immiscible.

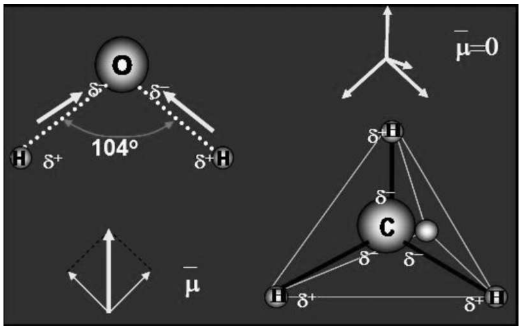

Figure 3: Intermolecular forces are electrostatic forces that are dependent on the molecular shapes.

Fowkes, Fowkes, 1972 has proposed an empirical relationship for the interfacial tension, σ_{ab}, between a polar and a non-polar liquid, where the cross mixing force, responsible for the interfacial tension reduction, is related to the dispersive components of the surface tensions, σ_a, σ_b, of each fluid through a geometrical average,

$$\sigma_{ab} = \sigma_a + \sigma_b - 2\sqrt{\sigma_a^d \sigma_b^d}. \tag{17}$$

The main idea behind Fowkes relation is displayed in Figure 4 where the cross mixing force is, in this case, of a pure dispersive nature.

When two drops of a liquid are close enough they will coalesce. Although the main coalescence driving force is the result of a collective electrostatic effect among the liquid molecules from both drops, the coalescence process is still an open problem, since vapor molecules near the contact point have theirs trajectories constrained by an intensified electrostatic field and, apparently, they preferentially condense on the positions where the liquid surfaces are closest, contributing to the start-up of coalescence. This picture was, indeed, observed in goniometer experiments (Figure 5), when two water drops coalesced in despite of their initial separation distance, of about 0.2 mm, was much larger than their electrostatic interaction length, but further theoretical studies are necessary for a more thorough analysis of this complex process.

When air displaces water inside a capilary channel, a dynamic liquid film forms separating the air phase from the solid surface. This dynamic liquid film has been studied by several authors including some famous ones such as Landau and Levich, 1942 and Bretherton, 1961. It has been shown that the average thickness of this film is dependent on the interface velocity, i.e., on the capillary number. When the air-water interface reaches very small constrictions of a porous medium, a pressure reduction in the invader phase, can give rise to

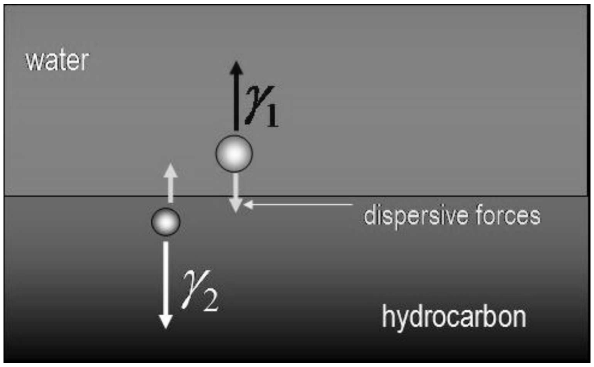

Figure 4: Dispersive forces try to mix water and oil.

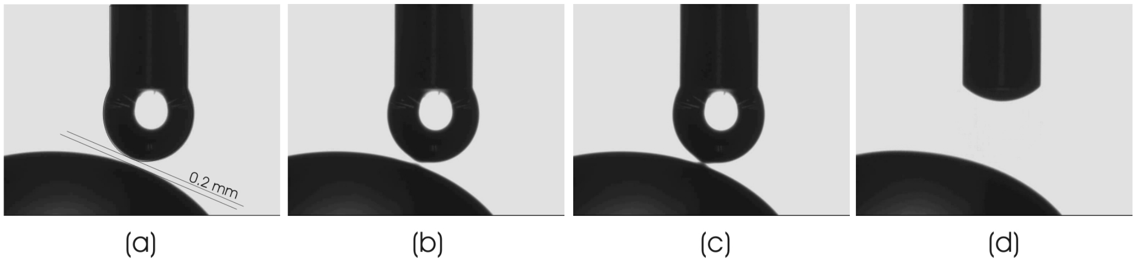

(a) (b) (c) (d)

Figure 5: Coalescence process between two water-droplets in a goniometer. The two drops coalesce after a certain time, although they were put at a distance of 0.2 mm, which is much larger than their electrostatic interaction length.

the growing of the film thickness followed by a coalescence process, breaking off the air phase and producing a burst of bubbles from the constriction due to the sucessive pressure decay followed by a pressure restoring after each coalescence process at the constriction. This is pictured in Figure 6.

This dynamical process can be very important in water flooding petroleum extraction, when the extraction is performed with a high capillary number or when the oil mobility is very low. In heavy oils, the presence of surfactants that are soluble in oil can give rise to stable emulsions.

In fact, the addition of surfactants that are soluble in the hydrocarbon phase will produce a polar cross mixing force and a larger decrease in the interfacial tension with respect to Eq. (17), in accordance with

$$\sigma_{ab} = \sigma_a + \sigma_b - 2\sqrt{\sigma_a^d \sigma_b^d} - 2\sqrt{\sigma_a^p \sigma_b^p}. \tag{18}$$

Surfactant molecules such as asphaltens can be pictured as in Figure 7(a), with a long hydrocarbon tail and a polar head. These molecules will move to the water-oil interface forming a monolayer where the molecule tails will be oriented toward the hydrocarbon phase, Figure 7(b).

Even when water wets the porous surface, when it displaces a heavy oil inside a porous medium, it is not able to produce a steady piston displacement, due to the high oil viscosity and water fingers will take form inside the oil-phase. These fingers are not stable and, in flowing through constrictions, they can break-up forming water drops, in the same manner as it was pictured in Figure 3. The presence of surfactants that are soluble in the oil phase, in the water-oil interface, reduces the interfacial tension making the break-up easier and the surfactant molecules will finish by forming a monolayer around each water droplet, difficulting the coalescence of these droplets and producing a stable emulsion in the downflow direction, Figure 7(c).

In concluding this section, in spite of its great technological importance and of the growing scientific interest in microhidrodynamics, the few physical problems that were drawn above give a sample of the great complexity with which we are faced, when trying to correct understand fluid flows, when the spatial scales are very small and when the interfacial physics play an important role.

In the next section the Boltzmann equation is presented, considered as a bridge that should enable to link the microscopic to the macroscopic scales.

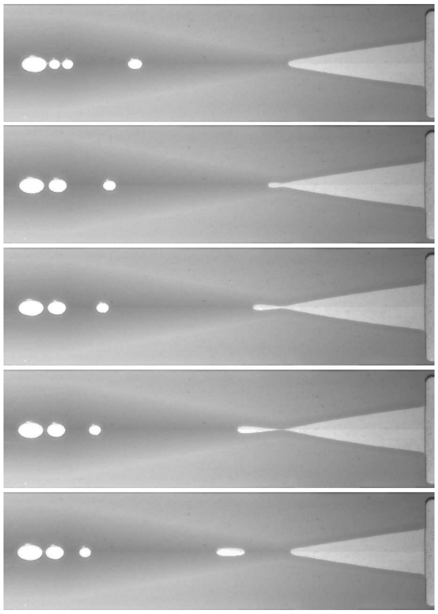

Figure 6: Formation of a burst of drops in a small constriction. Courtesy of O. Amyot, Amyot, 2004.

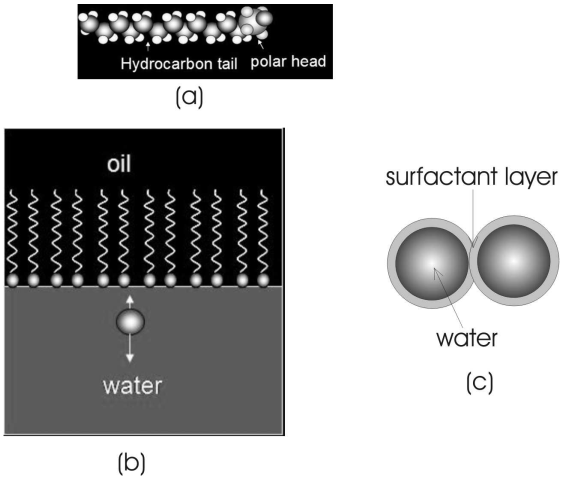

Figure 7: Surfactants and emulsions

4. Boltzmann equation as a bridge linking the molecular to the macroscopic domains

We first investigate the *origins* of the Boltzmann equation.

Figure 8 shows a molecular dynamics simulation of a vapor condensation process based on an N-body simulation of the Newton second law of motion. Each one of the N particles is subjected to a trajectory, in the physical space, given by the solution of the following equations

$$m_i \frac{d^2\vec{x}_i}{dt^2} = \sum_j F_{ij}, \tag{19}$$

$$\frac{d\vec{x}_i}{dt} = \vec{\mathsf{v}}_i, \tag{20}$$

where $\vec{x}_i$ is the position, $\vec{\xi}_i$ the velocity of particle i and F_{ij} is the force among each $i-$particle and all the remaining particles, evaluated by supposing a Lennard-Jones interaction potential among the particles, Surmas, 2006. Particles are spherical with a diameter that is given by the inversion point of the Lennard-Jones potential, where the attractive forces become repulsive. Each time a particle collide with the container surface, it is reflected back following a *specular* reflection and with only a previously established fraction of the kinetic energy it had before the collision, trying to reproduce a *cooling process* at the walls. Attractive forces between the wall container and the particles where not considered for avoiding condensation at the wall surface.

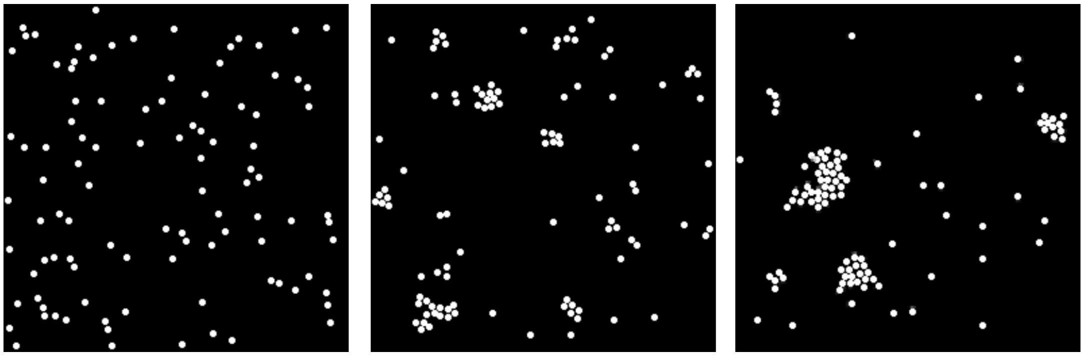

Figure 8: Molecular dynamics simulation of vapor condensation.

The initial state $\vec{x}_1, \vec{\xi}_1, ...\vec{x}_N, \vec{\xi}_N, t = 0$ was randomly set.

We can see that this molecular dynamics simulation gives a good picture of what is to happen in a condensation process at the molecular scale, although the analysis was performed on a *mechanical deterministic system of particles*, subjected to Newton 's second law of motion, without any help of thermodynamic concepts such as thermodynamic energy and entropy.

Nevertheless the results of such analysis is restricted: a) to the very small molecular scales and b) to very small time scales, considering the limitations imposed by the computer rounding-off error.

Consider, now our mechanical system of N particles, when several different initial state $\vec{x}_1, \vec{\xi}_1, ...\vec{x}_N, \vec{\xi}_N, t = 0$ are possible. Suppose that the set of all possible initial states is a dense set in the phase-space $\vec{x}_1, \vec{\xi}_1, ...\vec{x}_N, \vec{\xi}_N$. In this case it is impossible to know where a given particle will be at a given time. Let, however,

$$f^N\left(\vec{x}_1, \vec{\xi}_1, ...\vec{x}_N, \vec{\xi}_N, t\right), \tag{21}$$

to be the *probability* of finding, at time t, dt the particle 1 at the position $\vec{x}_1$, $d\vec{x}_1$ with velocity $\vec{\xi}_1$, $d\vec{\xi}_1$, the particle 2 at the position $\vec{x}_2$, $d\vec{x}_2$ with velocity $\vec{\xi}_2$, $d\vec{\xi}_2$ and so on, until particle N at the position $\vec{x}_N$, $d\vec{x}_N$ with velocity $\vec{\xi}_N$, $d\vec{\xi}_N$. The Liouville equation describing the dynamical evolution of this system is given by, Cercignani, 1969,

$$\partial_t f^N + \sum_i \vec{\xi}_i . \partial_{\vec{x}_i} f^N + \sum_i \vec{\chi}_i . \partial_{\vec{\xi}_i} f^N = 0, \tag{22}$$

where $\vec{\chi}_i$ is the force acting on particle i,

$$\vec{\chi}_i = \vec{\chi}_i^e + \sum_{\substack{j=1 \\ j \neq i}}^{N} \vec{\chi}_{ij}. \tag{23}$$

Force $\vec{\chi}_i^e$ is the force on particle i due to an external field and force $\vec{\chi}_{ij}$ is the force on particle i due to its interaction with particle j,

$$\vec{\chi}_{ij} = -\frac{\partial \Phi \left(x_{ij} \right)}{\partial \left(\vec{x}_i - \vec{x}_j \right)}, \tag{24}$$

where $x_{ij} = |\vec{x}_i - \vec{x}_j|$ and Φ is assumed to be a central potential depending, only, on the distance between particles i and j.

Conjoint probability f^N can be integrated in the phase space $\vec{x}_2, \vec{\xi}_2, ...\vec{x}_N, \vec{\xi}_N$ to give the marginal probability f^1 of finding, at time t, dt the particle 1 at the position $\vec{x}_1$, $d\vec{x}_1$ with velocity $\vec{\xi}_1$, $d\vec{\xi}_1$

$$f^1 \left(\vec{x}_1, \vec{\xi}_1, t \right) = \int ... \int f^N d\vec{x}_2 ... d\vec{x}_N d\vec{\xi}_2 ... d\vec{\xi}_N, \tag{25}$$

considering that the probability f^N gives a too detailed description of the system, which is unnecessarily complexe, since the dynamical evolution of an arbitrary, but, single, particle can be a reliable description of the whole mechanical system of particles, when these particles cannot be individually labelled.

After integration, considering $f = Nf^1$ the Liouville equation becomes, for large N,

$$\begin{aligned} \partial_t f + \vec{\xi}.\partial_{\vec{x}} f + \vec{\chi}^e.\partial_{\vec{\xi}} f &= -\partial_{\vec{\xi}} \int \int \vec{\chi}_{12} f^2 \left(\vec{x}_1, \vec{\xi}_1, \vec{x}_2, \vec{\xi}_2, t \right) d\vec{x}_2 d\vec{\xi}_2 = \frac{1}{m} \times \\ & \quad \partial_{\vec{\xi}} \int \int \frac{\partial \Phi \left(x_{12} \right)}{\partial \left(\vec{x}_1 - \vec{x}_2 \right)} f^2 \left(\vec{x}_1, \vec{\xi}_1, \vec{x}_2, \vec{\xi}_2, t \right) d\vec{x}_2 d\vec{\xi}_2 \end{aligned} \tag{26}$$

which is a Boltzmann equation for the distribution function f, with a collision term Ω. This collision term has been split in two collision terms, He and Doolen, 2002, $\Omega = \Omega^{sd} + \Omega^{ld}$, where Ω^{sd} is referred to short distance interactions, $|\vec{r}_1 - \vec{r}| < \sigma$ and Ω^{ld} to long range interactions $|\vec{r}_1 - \vec{r}| > \sigma$.

4.1. Long-range term

Consider, first, the long-range collision term

$$\begin{aligned} \Omega^{ld} &= \frac{\partial}{\partial \vec{\xi}}. \int \int_{|\vec{r}_1 - \vec{r}| > \varsigma} \frac{1}{m} \frac{\partial \phi \left(|\vec{r}_1 - \vec{r}| \right)}{\partial \left(\vec{r} \right)} \\ & \quad \times f^2 \left(\vec{r}, \vec{\xi}, \vec{r}_1, \vec{\xi}_1, t \right) d\vec{r}_1 d\vec{\xi}_1. \end{aligned} \tag{27}$$

By making the assumption that, for $|\vec{r}_1 - \vec{r}| > \sigma$, the molecular chaos prevails, He and Doolen, 2002,

$$f^2 \left(\vec{r}, \vec{\xi}, \vec{r}_1, \vec{\xi}_1 \right) = f \left(\vec{r}, \vec{\xi}, t \right) f \left(\vec{r}_1, \vec{\xi}_1, t \right) = f f_1, \tag{28}$$

one obtains,

$$\begin{aligned} \Omega^{ld} &= \frac{1}{m} \frac{\partial f \left(\vec{r}, \vec{\xi}, t \right)}{\partial \vec{\xi}} . \frac{\partial}{\partial \vec{r}} \int_{|\vec{r}_1 - \vec{r}| > \sigma} \phi \left(|\vec{r}_1 - \vec{r}| \right) \\ & \quad \times n \left(\vec{r}_1, t \right) d\vec{r}_1, \end{aligned} \tag{29}$$

The integrand in the above equation is the mean field, i.e., the field exerted by the n molecules placed at $\vec{r}_1 - \vec{r}$, on the molecules at position $\vec{r}$,

$$\phi_m\left(\vec{r}\right) = \int_{\left|\vec{r}_1-\vec{r}\right|>\sigma} \phi\left(\left|\vec{r}_1-\vec{r}\right|\right) n\left(\vec{r}_1,t\right) d\vec{r}_1 \tag{30}$$

Cosider $n\left(\vec{r}_1,t\right)$ to vary slowly with the spatial coordinate,

$$\begin{aligned} n\left(\vec{r}_1,t\right) &= n\left(\vec{r},t\right) + \nabla n.\left(\vec{r}_1-\vec{r}\right) + \\ \frac{1}{2}\nabla\nabla n &: \left[\left(\vec{r}_1-\vec{r}\right)\left(\vec{r}_1-\vec{r}\right)\right] + ..., \end{aligned} \tag{31}$$

In this case,

$$\phi_m\left(\vec{r}\right) = -an - \varkappa\nabla^2 n, \tag{32}$$

where

$$a \equiv -\int_{\dot{x}>\sigma} \phi\left(x\right) d\vec{x}, \tag{33}$$

$$\varkappa \equiv -\frac{1}{6}\int_{\dot{x}>\sigma} \phi\left(x\right) x^2 d\vec{x}, \tag{34}$$

because, $\phi < 0$.

With the above hypotheses, the long-range term can thus be written as

$$\Omega^{ld} = \frac{1}{m}\frac{\partial f\left(\vec{r},\vec{\xi},t\right)}{\partial\vec{\xi}}.\nabla\phi_m\left(\vec{r}\right). \tag{35}$$

4.2. Short-Range term

After some lengthy algebra, under the molecular chaos hypothesis and supposing that the collisions involve only a pair of particles, considered as material points, the short-range term collision term can be written as (Kremer, 2005),

$$\begin{aligned} \Omega^{sd} &= \int \left(f\left(\vec{r},\vec{\xi}',t\right) f\left(\vec{r},\vec{\xi}_1{}',t\right) - f\left(\vec{r},\vec{\xi},t\right) f\left(\vec{r},\vec{\xi}_1,t\right)\right) \\ &\quad \times gbdbd\epsilon d\vec{\xi}_1. \end{aligned} \tag{36}$$

This is the original Boltzmann collision term, (Boltzmann, 1866), deduced for material points, where $\vec{\xi}'$ and $\vec{\xi}_1'$ mean the velocities of, respectively, the target and the incident particles that rescue $\vec{\xi}$ and $\vec{\xi}_1$ after they collide, $\vec{g} = \vec{\xi}_1 - \vec{\xi}$ is the relative velocity and $g = \left|\vec{g}\right|$, b is an impact parameter related to the point where a particle, labeled as 1, reachs a spherical surface of radius σ around a target particle that moves, at the instant t, with the velocity $\vec{\xi}$ and ϵ is an azimuthal angle in the equatorial plane in the σ-sphere that is orthogonal to $\vec{\xi}_1 - \vec{\xi}$.

Enskog, Enskog, 1921, has, further, developed a collision model more appropriate for liquids, considering the particles to have a finite volume, since, in a liquid the mean free path has the same order of magnitude than the molecular diameter and multiple collisions are frequent, writting the collision term as

$$\begin{aligned} \Omega^{sd}_{Ensk} &= \int\int\int \left(\begin{array}{c} \chi\left(r+\frac{1}{2}\sigma\vec{k}\right) f\left(\vec{r},\vec{\xi}',t\right) f\left(\vec{r}+\sigma\vec{k},\vec{\xi}_1',t\right) - \\ \chi\left(r-\frac{1}{2}\sigma\vec{k}\right) f\left(\vec{r},\vec{\xi},t\right) f\left(\vec{r}-\sigma\vec{k},\vec{\xi}_1,t\right) \end{array} \right) \\ &\quad \times\sigma^2\vec{g}.\vec{k}d\vec{k}d\vec{\xi}_1 \end{aligned} \tag{37}$$

where

$$\vec{k} = (\cos\theta, \sin\theta\cos\epsilon, \sin\theta\sin\epsilon) \tag{38}$$

θ is a polar angle in the collision plane,

$$\theta = \arcsin\left(\frac{b}{\sigma}\right) \tag{39}$$

and χ is an *heuristic* correction factor introduced by Enskog to take account of the finite volume effects of the populations $f\left(\vec{r}, \vec{\xi}', t\right)$ and $f\left(\vec{r} + \sigma\vec{k}, \vec{\xi}_1{}', t\right)$.

5. Kinetic models for the collision term in the continuous velocity space

The collision term Ω is dependent on the distribution function itself and, indeed, the Boltzmann equation is a non-linear integro-differential equation. Instead of the full collision term, a collision model is required leading to a non-linear partial differential equation, which can be numerically solved. We restrict ourselves to the collision terms where the particles were considered without volume. The effect of the particle volume on discrete models, is, presently, still under investigation, He and Doolen, 2002, Surmas *et al.*, 2006.

5.1. BGK collision models

Considering the particles to be material points without volume and admitting the molecular chaos hypothesis, the collision term Ω in the Boltzmann equation, Eq. (1), was derived by Boltzmann in 1868 for binary collisions as Eq. (36).

The above hypothesis are only rigorously true for a rarefied gas without long-range attraction among their molecules. In addition, *molecular chaos* means that the post-collisional states of any two molecules are uncorrelated. If these hypothesis are accepted to be true, the Boltzmann equation is a non-linear integro-differential equation, which solution gives the distribution function $f(\vec{r}, \vec{c}, t)$, when the following molecular parameters are known: a) The molecular mass, m and b) the interaction potential, $\xi\left(|\vec{r}_1 - \vec{r}|\right)$. This means that any thermohydrodynamic problem could, in principle be solved, with solely these molecular informations and with appropriated boundary conditions. In fact, a Chapman-Enskog analysis of the Boltzmann equation with the collision term given by Eq. (36) shows that in the limit $Kn \to 0$, all the thermohydrodynamic equations are retrieved, with transport coefficients that are only dependent on the local physical state and on the above molecular properties.

Nevertheless, numerically solving this integro-differential equation has revealed to be a very complicated task. In addition, the full Boltzmann equation has details which are not, apparently, important, when the main worry is to describe the spatial and time evolution of the first hydrodynamic moments of the distribution function.

In this manner, consider replacing the collision term by a single relaxation term

$$\Omega = \frac{f^{eq} - f}{\tau}, \tag{40}$$

where τ is a relaxation time.

In spite of its apparent simplicity, Eq. (40) satisfy the main properties Eqs. (2-4) and the Boltzmann equation with the collision term given by Eq. (40) satisfy the H-theorem. Further, a Chapman-Enskog analysis shows that the full set of the thermohydrodynamic equations are retrieved with, nevertheless,

$$\frac{\mu}{2} = \frac{3\eta}{2} = \frac{3\varkappa}{10} = \frac{\rho e\tau}{3}, \tag{41}$$

leading to a non-manageable Prandtl number, due to the linear dependence of the viscosity coefficients and the thermal conductivity on the single relaxation parameter τ.

5.2. Deriving collision models with increased accuracy

Writting the distribution $f = f^{eq} + f^{neq}$, with $f^{neq} = f^{eq}\phi$, when f is near f^{eq} the short-range collision term can be written as

$$\Omega = f^{eq}\mathcal{L}(\phi), \tag{42}$$

where $\mathcal{L}$ is a linear operator, $\mathcal{L} : \xi^D \rightarrow \xi^D$.

For each point $\vec{r}$ the perturbation ϕ can be developed in terms of the Hermite polynomial tensors $\Psi_{\theta,(r_\theta)}$, Philippi *et al.*, 2006b, Shan and He, 1998,

$$\phi = \sum_{\theta} a^{\phi}_{\theta,(r_\theta)} \left(\vec{x}, t\right) \Psi_{\theta,(r_\theta)} \left(\vec{\mathcal{C}}_f\right), \tag{43}$$

and coefficients a^{ϕ}_{θ} can be related to the macroscopic moments of f. In this way, $a^{\phi}_{0} = 0$, $a^{\phi}_{1,\alpha} = 0$. The coefficient $a^{\phi}_{2,\alpha\beta}$ is related to the viscous stress tensor $\tau_{\alpha\beta}$ through

$$a^{\phi}_{2,\alpha\beta} = \frac{\tau_{\alpha\beta}}{2P}, \tag{44}$$

where $P = nkT$ is the thermodynamic pressure.

The peculiar kinetic energy $E(\vec{x}, t) = \rho e$ is given by

$$\rho e = \int f \frac{1}{2} m \left(\vec{c} - \vec{u}\right)^2 d\vec{c} = \int f^{eq} \frac{1}{2} m \left(\vec{c} - \vec{u}\right)^2 d\vec{c}. \tag{45}$$

In this way

$$\int f^{neq} \frac{1}{2} m C^2 d\vec{C} = 0, \tag{46}$$

or

$$\int f^{neq} \frac{1}{2} m C_\alpha C_\alpha d\vec{C} = \frac{1}{2} tr\left(\tau\right) = 0. \tag{47}$$

In two-dimensions

$$\tau_{xx} + \tau_{yy} = 0, \tag{48}$$

or

$$a^{\phi}_{2,xx} + a^{\phi}_{2,yy} = 0. \tag{49}$$

For third-order moments

$$\begin{aligned} S_{\alpha\beta\gamma} &= \int f m c_\alpha c_\beta c_\gamma d\vec{c} = \int f^{eq} m c_\alpha c_\beta c_\gamma d\vec{c} + \int f^{neq} m c_\alpha c_\beta c_\gamma d\vec{c} \\ &= S^{eq}_{\alpha\beta\gamma} + S^{neq}_{\alpha\beta\gamma}, \end{aligned} \tag{50}$$

with

$$S^{eq}_{\alpha\beta\gamma} = \rho u_\alpha u_\beta u_\gamma + P\left(\delta_{\beta\gamma} u_\alpha + \delta_{\alpha\gamma} u_\beta + \delta_{\alpha\beta} u_\gamma\right). \tag{51}$$

For the non-equilibrium part,

$$S^{neq}_{\alpha\beta\gamma} = \int f^{neq} m C_\alpha C_\beta C_\gamma d\vec{C} + \left(\tau_{\beta\gamma} u_\alpha + \tau_{\alpha\gamma} u_\beta + \tau_{\alpha\beta} u_\gamma\right), \tag{52}$$

resulting, using $a^{\phi}_{1,\alpha} = 0$, the invariance property with respect to index permutation and Eq. (51):

$$\begin{aligned} P\left(\frac{2kT}{m}\right)^{\frac{1}{2}} a^{\phi}_{3,\alpha\beta\gamma} &= \frac{S_{\alpha\beta\gamma}}{2} - \left[\begin{array}{c} \frac{1}{2}\rho u_\alpha u_\beta u_\gamma + \frac{1}{2} P\left(\delta_{\beta\gamma} u_\alpha + \delta_{\alpha\gamma} u_\beta + \delta_{\alpha\beta} u_\gamma\right) \\ + \frac{1}{2}\left(\tau_{\beta\gamma} u_\alpha + \tau_{\alpha\gamma} u_\beta + \tau_{\alpha\beta} u_\gamma\right) \end{array}\right] \\ &\equiv q_{\alpha\beta\gamma}. \end{aligned} \tag{53}$$

When β and γ are contracted, defining ϵ_α to be the total energy flux along the direction α,

$$P\left(\frac{2kT}{m}\right)^{\frac{1}{2}} a^{\phi}_{3,\alpha\beta\beta} = \epsilon_\alpha - \left[\frac{1}{2}\rho u^2 u_\alpha + P\left(\frac{D}{2} + 1\right) u_\alpha + \tau_{\alpha\beta} u_\beta\right] = q_\alpha, \tag{54}$$

where q_α is the *net* heat flux along the direction α, i.e., the total energy flux ϵ_α, excluding the flow of macroscopic kinetic energy $\frac{1}{2}\rho u^2 u_\alpha$, the compression work $P\left(\frac{D}{2}+1\right)u_\alpha$ and the viscous work $\tau_{\alpha\beta}u_\beta$.

Now, using the development, Eq. (43),

$$\mathcal{L}(\phi)=\sum_{\theta} a^{\phi}_{\theta,(r_\theta)}\mathcal{L}\left(\Psi_{\theta,(r_\theta)}\right). \tag{55}$$

The θ-order tensor $\mathcal{L}\left(\Psi_{\theta,(r_\theta)}\right)$ is, itself, an element of the $\mathcal{C}^D$ space and can be developed in terms of the θ-order Hermite tensors that belong to the orthogonal basis of this space,

$$\mathcal{L}\left(\Psi_{\theta,(r_\theta)}\right)=\sum_{(s_\theta)}\gamma_{(r_\theta),(s_\theta)}\Psi_{\theta,(s_\theta)}, \tag{56}$$

where $\gamma_{(r_\theta),(s_\theta)}$ designate the $(r_\theta),(s_\theta)$ components of 2θ-order *relaxation tensors.* As $\mathcal{L}$ is a self-adjoint operator, with non-positive eigenvalues, Cercignani, 1969,

$$\gamma_{(r_\theta),(m_\theta)}=\frac{\int e^{-\mathcal{C}_f^2}\mathcal{L}\left(\Psi_{\theta,(r_\theta)}\right)\Psi_{\theta,(m_\theta)}d\vec{\mathcal{C}}_f}{\int e^{-\mathcal{C}_f^2}\left(\Psi_{\theta,(m_\theta)}\right)^2 d\vec{\mathcal{C}}_f}\leq 0. \tag{57}$$

Using Einstein's notation

$$\mathcal{L}(\phi)=\sum_{\theta}\gamma_{(r_\theta),(s_\theta)}a^{\phi}_{\theta,(r_\theta)}\Psi_{\theta,(s_\theta)}, \tag{58}$$

where repeated indexes mean summation.

Above equation is an infinite summation on θ. When the terms above a chosen order N are diagonalised, following a Gross-Jackson procedure, Cercignani, 1969,

$$\mathcal{L}^{(N)}(\phi)=\sum_{\theta=0}^{N}\gamma_{(r_\theta),(s_\theta)}a^{\phi}_{\theta,(r_\theta)}\Psi_{\theta,(s_\theta)}-\gamma_{N+1}\sum_{\theta=N+1}^{\infty}\delta_{(r_\theta),(s_\theta)}a^{\phi}_{\theta,(r_\theta)}\Psi_{\theta,(s_\theta)}, \tag{59}$$

where

$$\delta_{(r_\theta),(s_\theta)}=\delta_{r_1 s_1}....\delta_{r_\theta s_\theta}. \tag{60}$$

In this way, using Eq. (43)

$$\mathcal{L}^{(N)}(\phi)=-\left[\sum_{\theta=0}^{N}\lambda_{(r_\theta),(s_\theta)}a^{\phi}_{\theta,(r_\theta)}\Psi_{\theta,(s_\theta)}\right]-\gamma_{N+1}\phi, \tag{61}$$

where $\lambda_{(r_\theta),(s_\theta)}=-\left(\gamma_{(r_\theta),(s_\theta)}+\gamma_{N+1}\delta_{(r_\theta),(s_\theta)}\right)$ is positive for all r_θ, s_θ, since a) $\lambda_{(r_\theta),(s_\theta)}=-\gamma_{(r_\theta),(s_\theta)}$ for all off-diagonal components and b) the diagonal components $\gamma_{(r_\theta),(r_\theta)}$ are negative with an absolute value that is greater than γ_{N+1} for all θ smaller or equal to N. Eq. (61) can be considered as an N^{th}-order kinetic model to the collision term, with an absorption term $\gamma_{N+1}\phi$ resulting from the diagonalization of the relaxation tensors after the given N. Therefore, all the moments of order higher than N are collapsed into a single non-equilibrium term minimizing the truncation effects on the fine structure of the $\mathcal{L}$-operator spectrum.

Eq. (61) generates increasing accuracy models to Ω when the distribution function f is near the Maxwell-Boltzmann equilibrium distribution, f^{eq}. Each term in the sum, in Eq. (61), gives the relaxation to the equilibrium of second or higher order kinetic moments M_θ that are not preserved in collisions, modulated by a λ_θ relaxation tensor.

5.2.1. A second order collision model in the two-dimensional space

Without any loss in the generality, we restrict ourselves to two-dimensional spaces and second order models, with $N=2$. In present section, the isotropy of 4^{th} rank tensors will be used to give explicit forms for the second-order collision model.

From Eq. (61)

$$\lambda_{(r_2),(s_2)}a^{\phi}_{2,(r_2)}\Psi_{2,(s_2)}=\lambda_{\alpha\beta\gamma\delta}a^{\phi}_{2,\alpha\beta}\Psi_{2,\gamma\delta}. \tag{62}$$

Requiring isotropy of 4^{th} rank tensors and considering the symmetry with respect to index permutation,

$$\lambda_{\alpha\beta\gamma\delta} = \lambda_{\mu}\left(\delta_{\alpha\beta}\delta_{\gamma\delta} + \delta_{\alpha\gamma}\delta_{\beta\delta} + \delta_{\alpha\delta}\delta_{\beta\gamma}\right). \tag{63}$$

In this way,

$$\begin{aligned} \lambda_{\alpha\beta\gamma\delta}a^{\phi}_{2,\alpha\beta}\Psi_{2,\gamma\delta} &= \lambda_{\mu}\left[a^{\phi}_{2,\alpha\alpha}\Psi_{2,\gamma\gamma} + a^{\phi}_{2,\alpha\beta}\Psi_{2,\alpha\beta} + a^{\phi}_{2,\alpha\beta}\Psi_{2,\beta\alpha}\right] \\ &= \lambda_{\mu}\left[\begin{array}{c} a^{\phi}_{2,xx}\left(\mathcal{C}^2_{fx} - \frac{1}{2}\right) + a^{\phi}_{2,yy}\left(\mathcal{C}^2_{fy} - \frac{1}{2}\right) + \\ 2a^{\phi}_{2,xy}\mathcal{C}_{fx}\mathcal{C}_{fy} \end{array}\right], \end{aligned} \tag{64}$$

since $a^{\phi}_{2,\alpha\alpha} = 0$. Using Eq.(44)

$$\lambda_{\alpha\beta\gamma\delta}a^{\phi}_{2,\alpha\beta}\Psi_{2,\gamma\delta} = \frac{\lambda_{\mu}}{P}\left[\tau_{xx}\left(\mathcal{C}^2_{fx} - \frac{1}{2}\right) + \tau_{yy}\left(\mathcal{C}^2_{fy} - \frac{1}{2}\right) + 2\tau_{xy}\mathcal{C}_{fx}\mathcal{C}_{fy}\right], \tag{65}$$

or, from Eq. (48), the second order model in two dimensions will be, finally, written as

$$\mathcal{L}^{(2)}(\phi) = -\frac{\lambda_{\mu}}{P}\left[\tau_{xx}\mathcal{C}^2_{fx} + \tau_{yy}\mathcal{C}^2_{fy} + 2\tau_{xy}\mathcal{C}_{fx}\mathcal{C}_{fy}\right] - \gamma_3\phi. \tag{66}$$

Present second-order continuous kinetic model is able for analyzing non-isothermal and fully compressible flows. The thermal conductivity is related to γ_3 diagonalization constant. Consideration of third-order collision models will be, only, necessary in multi-component systems, for correctly describing third-order coupling: the Soret and Dufour effects, Philippi and Brun, 1981a.

6. Velocity discretization

Discretization means to replace the entire continuous velocity space c^D by some discrete velocities $\vec{c}_i$. A Chapman-Enskog analysis shows that the correct macroscopic equations to be retrieved is given by assuring that the discrete distributions f_i^{eq} satisfy:

$$<\varphi_p>^{eq} = \int f^{eq}\left(\vec{\xi}\right)\varphi_p(\vec{\xi})d\vec{\xi} = \sum_i \frac{f_i^{eq}}{h^D}\varphi_p(\vec{\xi}_i), \tag{67}$$

for all $\{\varphi_p = 1, \xi_\alpha, \xi_\alpha\ \xi_\beta\ , \xi_\alpha\ \xi_\beta\ \xi_\gamma\ , ...\}$ of interest, where $f^{eq}\left(\vec{\xi}\right)$ is the MB distribution written in terms of the particles velocity $\vec{\xi}$ in the continuous space, h is the lattice unit, i.e., the smallest physical distance between any two contiguous grid points, D is the Euclidean dimension, $D = 2$ in the plane and $D = 3$ in three-dimnsional grids and $<\varphi_p>^{eq}$ means a macroscopic equilibrium moment of φ_p.

In Philippi *et al.*, 2006b, the discretization is considered as a quadrature problem, i.e., the discrete distributions f_i^{eq} in the right-hand side of Eq. (67) are replaced by $f^{eq}\left(\vec{\xi}_i\right)$, i.e., by the value of the MB distribution evaluated at the pole $\vec{\xi}_i$, multiplied by a parameter ω_i, which means the weight to be attributed to each velocity vector $\vec{\xi}_i$ for satisfying the quadrature condition, considering that, for each coordinate-axis α, the lattice-speeds $\xi_{i\alpha}$ form a discrete and finite set and the continuous velocity space is continuous and extends to infinity.

In this manner, the discretization restrictions, Eq. (67) are replaced by the following quadrature equations,

$$\begin{aligned} <\ \ &\varphi_p>^{eq} = \int f^{eq}\left(\vec{\xi}\right)\varphi_p(\vec{\xi})d\vec{\xi} \\ =\ \ &\sum_i \omega_i\left(\frac{2kT_0}{m}\right)^{D/2} f^{eq}\left(\vec{\xi}_i\right)\varphi_p(\vec{\xi}_i), \end{aligned} \tag{68}$$

where the factor $\left(\frac{2kT_0}{m}\right)^{D/2}$ was introduced for assuring ω_i to be a dimensionless, real number, since $f^{eq}\left(\vec{\xi}\right)$ is the number of particles per unit volume of the velocity space and per unit volume of the physical space.

When performing the quadrature, an integration variable must be chosen. If the dimensionless fluctuation velocity $\vec{\mathcal{C}}_f = \frac{\vec{\xi}-\vec{u}}{\left(\frac{2kT}{m}\right)^{1/2}}$ is chosen as the integrating variable, the particle velocities result dependent on T and on $\vec{u}$, Philippi *et al.*, 2006b,

$$\vec{\xi}_i = \vec{u} + \left(\frac{2kT}{m}\right)^{1/2} \vec{\mathcal{C}}_{fi} = \vec{\xi}_i \left(T, \vec{u}\right). \tag{69}$$

Another choice is the dimensionless particle velocity $\vec{\mathcal{C}} = \frac{\vec{c}}{\left(\frac{2kT}{m}\right)^{1/2}}$. In this case, the particle velocities are temperature dependent, Philippi *et al.*, 2006b,

$$\vec{\xi}_i = \left(\frac{2kT}{m}\right)^{1/2} \vec{\mathcal{C}}_i = \vec{\xi}_i \left(T\right). \tag{70}$$

Avoiding the $\vec{\xi}_i$ temperature dependence requires to consider the particles velocity $\vec{\xi}$ as the integrating variable when performing the quadrature, i.e., to let c^2 free from T in the exponential part $e^{-\mathcal{C}^2}$of the equilibrium distribution. This can be accomplished by writing, Philippi *et al.*, 2006b, Shan and He, 1998,

$$e^{-\frac{(c-u)^2}{\frac{2kT}{m}}} = \left(e^{-\mathcal{C}_{fo}^2}\right)^{\frac{T_0}{T}}, \tag{71}$$

where T_0 is a reference (and constant) temperature and $\vec{\mathcal{C}}_{fo} = \frac{\vec{\xi}-\vec{u}}{\left(\frac{2kT_0}{m}\right)^{1/2}}$ is a new dimensionless peculiar velocity referred to the temperature T_o.

When T is near T_0, i.e., when the departures from thermal equilibrium are small, the above expression may be developed in a Taylor series around $\frac{T}{T_o} = 1$. Considering $\Theta = \frac{T}{T_o} - 1$ to be the temperature deviation, this development gives

$$\left(e^{-\mathcal{C}_{fo}^2}\right)^{\frac{T_0}{T}} = e^{-\mathcal{C}_{fo}^2}\left[1 + \mathcal{C}_{fo}^2\Theta + \frac{1}{2}\mathcal{C}_{fo}^2\left(\mathcal{C}_{fo}^2 - 2\right)\Theta^2 + ...\right], \tag{72}$$

which terms are increasing powers of $\mathcal{C}_{fo}^2$.

Consider writing the MB equilibrium distribution as

$$\begin{aligned} f^{eq} &= n_d\left(\frac{m}{2\pi kT}\right)^{D/2} e^{-\mathcal{C}_f^2} \\ &= n_d\left(\frac{m}{2\pi kT}\right)^{D/2} e^{-\mathcal{C}_{fo}^2}\left[1 + \mathcal{C}_{fo}^2\Theta + \frac{1}{2}\mathcal{C}_{fo}^2\left(\mathcal{C}_{fo}^2 - 2\right)\Theta^2 + ...\right] \\ &= n_d\left(\frac{m}{2\pi kT}\right)^{D/2} e^{-\mathcal{C}_o^2} e^{-\mathcal{U}_o^2 + 2\vec{\mathcal{U}}_o.\vec{\mathcal{C}}_o} \\ &\quad \times\left[1 + \mathcal{C}_{fo}^2\Theta + \frac{1}{2}\mathcal{C}_{fo}^2\left(\mathcal{C}_{fo}^2 - 2\right)\Theta^2 + ...\right]. \end{aligned} \tag{73}$$

The exponential term $e^{-\mathcal{U}_o^2 + 2\vec{\mathcal{U}}_o.\vec{\mathcal{C}}_o}$ is the generating function of the Hermite polynomials $\Psi_{\theta,(r_\theta)}\left(\vec{\mathcal{C}}_o\right)$ in the velocity space, where (r_θ) is a sequence of indexes $r_1, r_2, ...r_\theta$,

The Hermite tensors are orthogonal in the Hilbert space $\mathcal{H}$, with respect to the inner product

$$\left(h * g\right)_c = \frac{1}{\pi^{D/2}}\int e^{-\mathcal{C}^2} hg d\vec{\mathcal{C}}, \tag{74}$$

and symmetric wih respect to any index permutation.

After some straightforward algebra, the result for the equilibrium distribution can then be written as an infinite series, Philippi *et al.*, 2006b,

$$f^{eq}=\frac{1}{\pi^{D/2}}\left(\frac{m}{2kT_0}\right)^{D/2}e^{-\mathcal{C}_0^2}\sum_{\theta}a^{eq}_{\theta,(r_\theta)}\left(n_d,\vec{\mathcal{U}}_0,\Theta\right)\Psi_{\theta,(r_\theta)}\left(\vec{\mathcal{C}}_o\right). \tag{75}$$

where the coefficients $a^{eq}_{\theta,(r_\theta)}$ are related, respectively, to the f macroscopic properties, at equilibrium: the number density of particles, n_d, the local momentum, $n_d\mathcal{U}_{0,\alpha}$, the momentum flux, $\Pi^{eq}_{\alpha\beta}$, the energy flux, $e^{eq}_{\alpha\beta\gamma}$ and an hyper-flux of momentum, $\Xi^{eq}_{\alpha\beta\gamma\delta}$.

From Eq. (68), it is easy to see that its corresponding discrete form can be written as,

$$f_i^{eq}=W_i\sum_{\theta}a^{eq}_{\theta,(r_\theta)}\left(n,\vec{\mathcal{U}}_0,\Theta\right)\Psi_{\theta,(r_\theta)}\left(\vec{\mathcal{C}}_{o,i}\right). \tag{76}$$

where $n=n_dh^D$ and $W_i=\frac{1}{\pi^{D/2}}\omega_i e^{-\mathcal{C}_{0,i}^2}$, Philippi *et al.*, 2006b.

Consider the inner products in the continuous and discrete space, given respectively by,

$$(f*g)_c\equiv\frac{1}{\pi^{D/2}}\int e^{-\mathcal{C}_0^2}fg\,d\vec{\mathcal{C}}_0, \tag{77}$$

$$(f*g)_d\equiv\sum_i W_i f\left(\vec{\mathcal{C}}_{o,i}\right)g\left(\vec{\mathcal{C}}_{o,i}\right), \tag{78}$$

where $W_i=\frac{1}{\pi^{D/2}}\omega_i e^{-\mathcal{C}_{0i}^2}$ and their induced norms

$$\|f\|_c^2\equiv\frac{1}{\pi^{D/2}}\int e^{-\mathcal{C}_0^2}f^2d\vec{\mathcal{C}}_0, \tag{79}$$

$$\|f\|_d^2\equiv\sum_i W_i f^2\left(\vec{\mathcal{C}}_{o,i}\right). \tag{80}$$

Since functions $\Psi_{\theta,(r_\theta)}\left(\vec{\mathcal{C}}_o\right)$ are orthogonal in the continuous space with respect to the inner product Eq. (77), it can be shown, Philippi *et al.*, 2006b, that the quadrature equation, Eq. (68) requires the orthogonality of $\Psi_{\theta,(r_\theta)}\left(\vec{\mathcal{C}}_{o,i}\right)$ and their norm preservation in the discrete space, i.e.,

$$\sum_i W_i\Psi^2_{\theta,(r_\theta)}\left(\vec{\mathcal{C}}_{o,i}\right)=\frac{1}{\pi^{D/2}}\int e^{-\mathcal{C}_0^2}\Psi^2_{\theta,(r_\theta)}\left(\vec{\mathcal{C}}_o\right)d\vec{\mathcal{C}}_o \tag{81}$$

In this manner, the still unknown weights W_i and the discrete velocities $\vec{\mathcal{C}}_{o,i}$ must be chosen in such a manner that the orthogonality of the Hermite polynomial tensors $\Psi_{\theta,(r_\theta)}$ is assured in the discrete space and satisfying the norm preservation equation, Eq. (81). In Philippi *et al.*, 2006b, it is shown that the norm preservation equation warrants the orthogonality of $\Psi_{\theta,(r_\theta)}\left(\vec{\mathcal{C}}_{o,i}\right)$, with respect to the inner product, Eq. (78), when the discrete velocity space is a *Bravais* lattice.

The above conclusion is very important because it reduces our discretization problem to find the weights W_i and the poles $\vec{\mathcal{C}}_{oi}$ satisfying, solely, the norm restrictions, Eq. (81).

With the exception of a very few lattices, Gaussian-like quadratures does not give a regular discrete set $\vec{\mathcal{C}}_{oi}$. Nevertheless, if any Bravais velocity set $\{\vec{e}_i\}$, giving a space-filling lattice, is chosen, the quadrature problem can be considered as to find the weights W_i and a scaling factor a such that $\vec{\mathcal{C}}_{o,i}=a\vec{e}_i$, satisfying Eq. (81). Considering that the poles $\vec{e}_i$ are previously known, this quadrature method was named as *quadrature with prescribed abcissae,* Philippi *et al.*, 2006b.

In this way, when the order of approximation N of the Hermite polynomial expansion to the MB equilibrium distribution is chosen, a set $\Psi_{\theta,(r_\theta)}$, $\theta=0,...,N$, is established, and the infinite and enumerable basis of the Hilbert space $\mathcal{H}:c^D\rightarrow\mathcal{R}$, which generates the solutions of the continuous Boltzmann equation, is replaced by a *finite* set of Hermite polynomial tensors, restricting the solutions to N^{th}-degree polynomials in the velocity $\vec{c}$. The quadrature problem is, now, to select a regular lattice $\{\vec{e}_i\}$, in such a manner that functions $\Psi_{\theta,(r_\theta)}$

preserve the orthogonality with respect to the inner product in the discrete space and this can be accomplished by assuring that the norm of *each one* of these functions $\Psi_{\theta,(r_\theta)}$ is retrieved, *exactly*, in the discrete space. The number b of the required lattice vectors is proportional to the order N of the polynomial approximation, $b = b(N)$. In addition, we have shown, Philippi *et al.*, 2006b, that when the quadrature problem is solved, the 2θ-rank tensors given by,

$$\Lambda_{(r_\theta),(s_\theta)} = \sum_i W_i \mathcal{C}_{0,i,r_0} ... \mathcal{C}_{0,i,r_\theta} \mathcal{C}_{0,i,s_0} ... \mathcal{C}_{0,i,s_\theta}, \tag{82}$$

are *isotropic* in the discrete space, for $\theta = 1, ...N$.

6.1. Two-dimensional square lattices

We restrict our attention to two-dimensional square lattices, in this work, although the above presented quadrature procedure is general and may be used for deriving two and three-dimensional lattices.

The dimensionless local velocity

$$\vec{\mathcal{U}}_0 = \frac{\vec{u}}{\left(\frac{2kT_0}{m}\right)^{1/2}}, \tag{83}$$

can be scaled for enabling to work with unitary lattice-units. In this manner, the spatial and the time scales, respectively, h and δ, can be chosen so as to satisfy,

$$\frac{h}{\delta} = \left(\frac{2kT_0}{m}\right)^{1/2}, \tag{84}$$

and, since

$$n\vec{\mathcal{U}}_0 = \sum_i f_i \vec{\mathcal{C}}_{oi} = a \sum_i f_i \vec{e}_i, \tag{85}$$

where $\vec{e}_i$ are the usual lattice vectors in 2D lattices, a new local velocity can be defined as

$$n\vec{u}^* = \frac{n\vec{\mathcal{U}}_0}{a} = \sum_i f_i \vec{e}_i. \tag{86}$$

In two dimensions, square lattices like the D2Q9, D2Q13,..., have four discrete velocities at each energy level $\mathcal{C}_o$. Figure 9 summarizes some square lattices that are being used in lattice-Boltzmann simulation: each set of four discrete velocities is superposed to the previous lattice-vectors set when adding a single energy level, following the sequence $\left(0,\ 1,\ \sqrt{2},\ 2,\ 2\sqrt{2},\ 3,\ 3\sqrt{2},...\right)$.

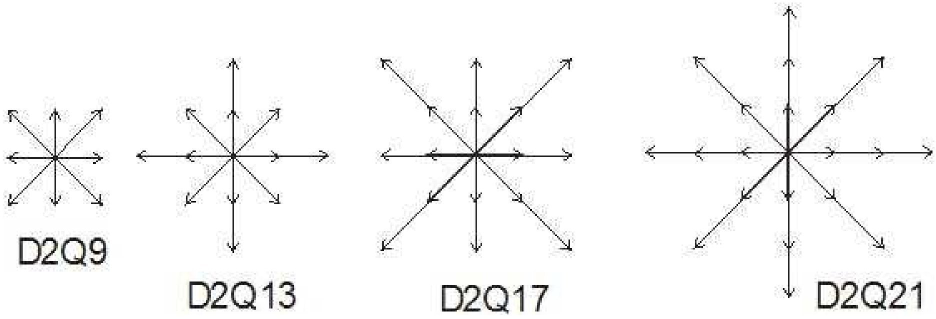

Figure 9: Some two-dimensional square lattices that are usual in LBM.

When $N = 2$ there will be 4 linearly independent equations for 4 unknowns related to the scaling factor a, and the D2Q9 weights W_0, W_1,W_2. This set has a unique solution leading to the widely known values $W_0 = 16/36$, $W_1 = 4/36$,$W_2 = 1/36$ and $a = \sqrt{3/2}$.

The equilibrium distribution for the D2Q9 lattice is, then,

$$f_{i,2}^{eq} = W_i n \left(\begin{array}{c} 1 + 2a^2 u_\alpha^* e_{i,\alpha} + 2a^2 u_\alpha^* u_\beta^* \left(a^2 e_{i,\alpha} e_{i,\beta} - \frac{1}{2}\delta_{\alpha\beta}\right) + \\ \Theta \left(a^2 e_i^2 - 1\right) \end{array} \right), \tag{87}$$

with third-order errors $\mathcal{O}(\Theta u^*, u^{*3})$, with respect to the full MB distribution.

The effect of temperature on the equilibrium distribution can be clearly seen from Eq. (87). In higher temperature sites, the amount of rest particles is reduced and redistributed to higher energy levels, trying to mimic the temperature dependence of the continuous MB distribution. This effect is highly desirable in thermal LBE simulation. An equilibrium distribution similar to Eq.(87) is given as Eq. (18) of Shan and He, 1998.

The D2Q13 and the next lattices are also able to run second-order models. In these cases, the number of unknowns is greater than the number of disposable equations and several solutions will be available, satisfying the quadrature problem.

Nevertheless, contrary to MacNamara and Alder results (McNamara and Alder, 1993) and to the results that would be expected with fitting methods, this lattice is *not able* to run *full* third order models. Indeed, when $N = 3$, it is impossible to find real positive values for a, W_0, W_1,W_2, W_3 satisfying all the norm restrictions, Eq. (81) related to $\Psi_{3,\alpha\beta\gamma}$. This result is the same for the D2Q17 lattice.

Considering the D2Q21 lattice as a next candidate for third order models, there will be, in this case, 7 unknowns a, W_0, W_1,W_2, W_3,W_4, W_5 for 6 norm restrictions, after eliminating identical equations. Letting a to be a free variable, the system gives a solution with real positive roots when a is inside the interval $0.659\,836 \leq a \leq 1.16208$.

The values $a = 0.659\,836$ and $a = 1.16208$ (in fact, $a = \frac{1}{12}\sqrt{5}\sqrt{\sqrt{193} + 25}$) are roots of the polynomials $W_0(a)$ and $W_3(a)$, respectively. In this manner, when the value $a = 1.16208$ is chosen, $W_3 = 0$ and the lattice loss an energy level, giving a modification of the D2Q17 lattice, which has been named D2V17, shown in Figure 10. The weights, with six significant digits, are $W_0 = 0.402005$, $W_1 = 0.116155$, $W_2 = 0.0330064$, $W_3 = 0$, $W_4 = 0.0000790786$, $W_5 = 0.000258415$.

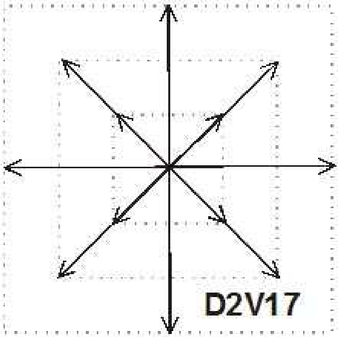

Figure 10: The D2V17 lattice.

This modified square lattice is less expensive considering computer requirements and has the same properties when compared with the D2Q21 lattice, i.e., it retrieves, exactly, all the equilibrium moments up to the 3^{rd} order and ii) gives isotropic tensors up to the 6^{th} rank. Therefore, present method can be, also, considered as a tool for investigating the structure of minimal velocity sets giving regular lattices.The D2V17 equilibrium distribution can be written as

$$\begin{aligned} f_{i,3}^{eq} &= f_{i,2}^{eq} + W_i a_{3,\alpha\beta\gamma}^{eq} \Psi_{3,\alpha\beta\gamma}(i) = \\ & W_i n \left[\begin{array}{c} 1 + 2a^2 u_\alpha^* e_{i,\alpha} + 2\left(a^2 u_\alpha^* u_\beta^*\right)\left(a^2 e_{i,\alpha} e_{i,\beta} - \frac{1}{2}\delta_{\alpha\beta}\right) + \\ \Theta\left(a^2 e_i^2 - 1\right) \\ + \frac{4}{3} a^3 u_\alpha^* u_\beta^* u_\gamma^* \left[\begin{array}{c} a^3 e_{i,\alpha} e_{i,\beta} e_{i,\gamma} - \\ \frac{a}{2}\left(e_{i,\alpha}\delta_{\beta\gamma} + e_{i,\beta}\delta_{\alpha\gamma} + e_{i,\gamma}\delta_{\alpha\beta}\right) \end{array} \right] \\ + 2\Theta a^2 \left(a^2 e_i^2 - 2\right) u_\gamma^* e_{i,\gamma} \end{array} \right], \end{aligned} \tag{88}$$

with fourth-order errors $\mathcal{O}(\Theta u^{*2}, u^{*4})$.

In addition to the equilibrium moments up to order 3, thermohydrodynamics requires the 4^{th}-order equilibrium moments $< \mathcal{C}_0^2\mathcal{C}_{0,x}^2 >^{eq}$, $< \mathcal{C}_0^2\mathcal{C}_{0,y}^2 >^{eq}$and $< \mathcal{C}_0^2\mathcal{C}_{0,x}\mathcal{C}_{0,y} >^{eq}$to be retrieved, McNamara and Alder, 1993. Since these functions are not orthogonal in the continuous velocity space, a Gram-Schmidt orthogonalization procedure was used to find orthogonal polynomials from this set by using the previous Hermite polynomials and the inner product Eq. (77).

The result was

$$\Psi_{4,1} = \mathcal{C}_o^2\mathcal{C}_{o,x}^2 - \frac{7}{2}\mathcal{C}_{o,x}^2 - \frac{1}{2}\mathcal{C}_{o,y}^2 + 1, \tag{89}$$

$$\Psi_{4,2} = \frac{1}{7}\left(\mathcal{C}_o^2\left(7\mathcal{C}_{o,y}^2 - \mathcal{C}_{o,x}^2\right) - 24\mathcal{C}_{o,y}^2 + 6\right), \tag{90}$$

$$\Psi_{4,3} = \mathcal{C}_{o,x}\mathcal{C}_{o,y}\left(\mathcal{C}_o^2 - 3\right). \tag{91}$$

When we require the norm preservation of the functions $\Psi_{4,1}$, $\Psi_{4,2}$ and $\Psi_{4,3}$ this gives a system of 8 independent equations for 9 unknowns. In this case, a is, again, a free parameter and the solution gave real positive weights for $0.590193 \leq a \leq 0.760569$.

Further, when a is, respectively, taken as 0.590193 or 0.760569 the weights W_1 or W_6 are null, giving two D2V25 lattices that retrieve the correct thermohydrodynamics equations. These lattices are shown in Figure 11. For the first lattice, called D2V25(W1), $a = 0.590193$ and the calculated weights are $W_0 = 0.235184$, $W_1 = 0$, $\mathrm{W}_2 = 0.101\,817$, $W_3 = 5.921\,34 \times 10^{-2}$, $W_4 = 2.004\,09 \times 10^{-2}$, $W_5 = 6.795\,23 \times 10^{-3}$, $W_6 = 1.143\,76 \times 10^{-3}$, $W_7 = 2.197\,88 \times 10^{-3}$. Lattice D2V25(W6) has $a = 0.760569$ and $W_0 = 0.239\,059$, $W_1 = 0.063\,158$, $W_2 = 8.759\,57 \times 10^{-2}$, $W_3 = 3.118\,00 \times 10^{-2}$, $W_4 = 6.198\,96 \times 10^{-3}$, $W_5 = 2.020\,13 \times 10^{-3}$, $W_6 = 0$, $W_7 = 8.382\,24 \times 10^{-5}$.

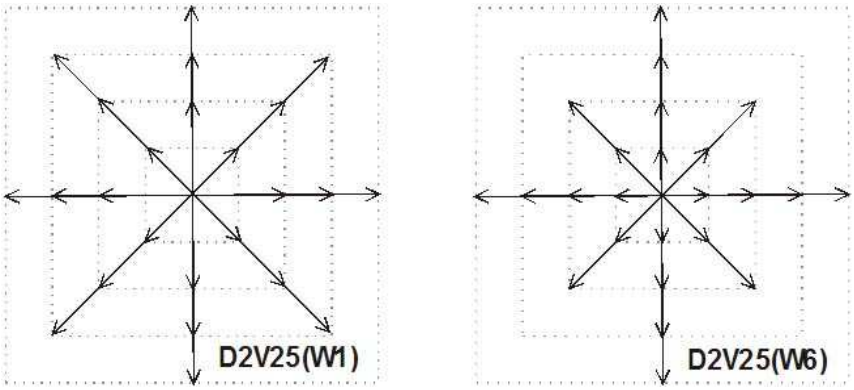

Figure 11: The D2V25 lattices for thermal problems.

Therefore, thermohydrodynamic equations are correctly retrieved with the LBE based on these lattices, but isotropy of 8^{th}-rank tensors cannot be assured. The equilibrium distribution for this lattice can be written as

$$f_{i,th}^{eq} = f_{i,3}^{eq} + W_i\left[a_{4,1}^{eq}\Psi_{4,1}(i) + a_{4,2}^{eq}\Psi_{4,2}(i) + a_{4,3}^{eq}\Psi_{4,3}(i)\right], \tag{92}$$

with, nevertheless, fourth-order errors $\mathcal{O}(\Theta u^{*2}, u^{*4}, \Theta^2)$ with respect to the full MB distribution. Parameters $a_{4,\theta}^{eq}$ can be found by using the orhogonality properties of $\Psi_{4,\theta}\left(\vec{\mathcal{C}_0}\right)$ in the continuous space, giving,

$$a_{4,1}^{eq} = \frac{2}{7}\left(2a^4u_x^{*2}u^{*2} + \Theta a^2\left(6u_x^{*2} + u^{*2}\right) + 2\Theta^2\right), \tag{93}$$

$$a_{4,2}^{eq} = \frac{1}{12}\left(7a^4u_y^{*4} + a^4u_x^{*4} + 6a^4u_x^{*2}u_y^{*2} + 24a^2u_y^{*2}\Theta + 6\Theta^2\right), \tag{94}$$

$$a^{eq}_{4,3} = \frac{4}{3} a^2 u_x^* u_x^* \left(3\Theta + a^2 u^2\right).$$

For full fourth-order model, the norm preservation of a full set of Hermite orthogonal polynomials until the 4^{th}-order is required, giving a set of 9 norm restrictions. This system will be, only, closed for a lattice with 8 energy levels. The D2Q29 lattice, with 8 weights $\mathrm{W}_0, ..., \mathrm{W}_7$, is a natural candidate to be the *minimal* square lattice to run fourth-order models in the square lattices hierarchy. For this lattice, there are 9 linearly independent equations. This closed set of 9 independent equations has, nevertheless, no solution.

This result was the same for the next D2Q33 lattice, when a is let as a free parameter.

Since each function $\Psi_{\theta,(r_\theta)}$ is a linear combination of the monomials $\varphi = \left\{1, \mathcal{C}_{ox}, \mathcal{C}_{oy}, \mathcal{C}_{ox}^2, \mathcal{C}_{oy}^2, \mathcal{C}_{ox}\mathcal{C}_{oy}, ...\right\}$, the norm restrictions, Eq. (81), can be indifferently used on the set Ψ of orthogonal functions or on set φ of monomials. The last choice is, in present case, preferable, for identifying a symmetry overcome in the Q-series hierarchy of square lattices (Figure 9). Indeed, consider the fourth-order functions $\varphi_{4,1} = \mathcal{C}_{oy}^2 \mathcal{C}_{ox}^2$ and $\varphi_{4,2} = \mathcal{C}_{ox}^3 \mathcal{C}_{oy}$. These functions have different norms in the continuous space, respectively, $\frac{3}{4}$ and $\sqrt{\frac{15}{16}}$. Nevertheless, since $\varphi_{4,1} = \left(\mathcal{C}_{oy}\mathcal{C}_{ox}\right)^2$ and $\varphi_{4,2} = \left(\mathcal{C}_{ox}\mathcal{C}_{oy}\right)\mathcal{C}_{ox}^2$ the only contributions for their norms, in the discrete space, came from the diagonal vectors and are the same, because, along these directions, $\mathcal{C}_{o,iy} = \mathcal{C}_{o,ix}$.

This is an important result, since it means that the Q-series of square lattices are unable to run full fourth-order LBE models.

In this way, we have tried another building structure for the lattices, filling completely the available Cartesian space around each site, following the sequence $|e_i| = 0,\ 1,\ \sqrt{2},\ 2,\ \sqrt{5},\ 2\sqrt{2},\ 3,\ \sqrt{10}$ with sequentially increasing values for $|e_i|$.

Figure 12 shows a D2V37 lattice, constructed in such a manner, with 37 velocity vectors, but 8 weights W_i. Solution of the 9 norm equations is unique and gives, when 6 significant digits are considered, $a = 0.846393$, $W_0 = 0.233151$, $W_1 = 0.107306$, $W_2 = 0.0576679$, $W_3 = 0.0142082$, $W_4 = 0.00535305$, $W_5 = 0.00101194$, $W_6 = 0.000245301$, $W_7 = 0.000283414$. This lattice came from the solution of a closed system with 9 linearly independent norm restriction for 9 unknowns.

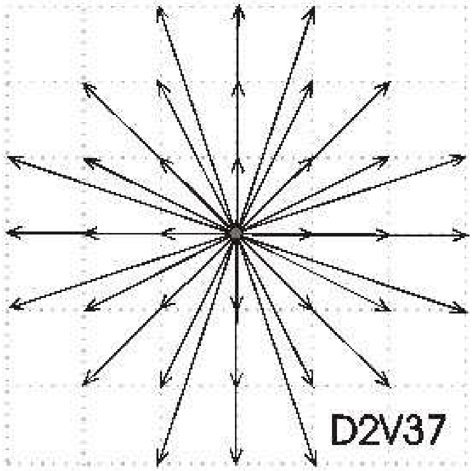

Figure 12: The D2V37 lattice.

Since, in the D2V37 lattice, all the fourth-order Hermite polynomial tensors belong to the orthogonal basis of this lattice, the equilibrium distribution can be written as,

$$
\begin{aligned}
f^{eq}_{i,4} &= f^{eq}_{i,3} + W_i a^{eq}_{4,\alpha\beta\gamma\delta}\Psi_{4,\alpha\beta\gamma\delta}(i) = \\
& W_i n \left\{ \begin{array}{c}
1 + 2a^2 u^*_\alpha e_{i,\alpha} + 2\left(a^2 u^*_\alpha u^*_\beta\right)\left(a^2 e_{i,\alpha}e_{i,\beta} - \frac{1}{2}\delta_{\alpha\beta}\right) \\
+\Theta\left(a^2 e_i^2 - 1\right) \\
+\frac{4}{3} a^3 u^*_\alpha u^*_\beta u^*_\gamma \left[\begin{array}{c} a^3 e_{i,\alpha}e_{i,\beta}e_{i,\gamma} \\ -\frac{a}{2}\left(e_{i,\alpha}\delta_{\beta\gamma}+e_{i,\beta}\delta_{\alpha\gamma}+e_{i,\gamma}\delta_{\alpha\beta}\right)\end{array}\right] \\
+2\Theta a^2\left(a^2 e_i^2 - 2\right) u^*_\gamma e_{i,\gamma} + \\
\frac{2}{3}\left[\begin{array}{c}
\left[a^8\left(u^*_\alpha e_{i\alpha}\right)^4 - 3a^6 u^{*2}\left(u^*_\alpha e_{i\alpha}\right)^2 + \frac{3}{4}a^4 u^{*4}\right] + \\
\Theta\left[\begin{array}{c}
3a^6\left(u^*_\alpha e_{i\alpha}\right)^2 e_i^2 - \\
\frac{3}{2}a^4\left(D\left(u^*_\alpha e_{i\alpha}\right)^2 + 4\left(u^*_\alpha e_{i\alpha}\right)^2 + u^{*2}e_i^2\right) + \\
\frac{3}{4}a^2 u^{*2}\left(D+2\right)
\end{array}\right] \\
+\frac{3}{4}\Theta^2\left[a^4 e_i^4 - \frac{1}{2}a^2\left(D+2\right)e_i^2 + \frac{1}{4}D\left(D+2\right)\right]
\end{array}\right]
\end{array}\right\}.
\end{aligned}
\tag{95}
$$

The D2V37 lattice, with the above equilibrim distribution, can be considered as the *minimal* square lattice giving a fourth-order approximation to the continuous Boltzmann equation, wih errors $\mathcal{O}\left(\Theta^2 u^*, u^{*5}\right)$.

The weights W_i, in general, decrease with i and attain very small values when i is large. The smallness of W_i for large i is expected and is a consequence of: a) the restriction that was imposed on the lattice to be space filling, requiring the norm of each added lattice-vector, $\vec{e}_i$ to be, frequently, an integer multiple of the norm of the lattice-vectors forming the D2Q9 lattice unitary-cell, in square-lattices; b) the required degree of approximation leading to polynomials with terms of $\mathcal{O}\left(e_b^N\right)$.

7. Immiscible fluids

Flow of immiscible fluids is, classically, treated in fluid mechanics by considering that the transition layer has a null thickness and by performing a momentum balance around this layer. At microscopic level, when two immiscible fluids r and b are mixed, the long-range attraction between the molecules of each fluid is the molecular mechanism promoting fluid segregation. Intermolecular forces may be of many different types, including electrostatic forces between permanent dipoles, induction forces between permanent dipoles and induced dipoles, dispersion forces between non-polar molecules and hydrogen bonds. In the transition region between the two fluids, a molecule is, predominantly, subjected to attractive fields from its own phase that acts as a potential barrier and gives rise to fluid-fluid interfacial tension. In addition, molecules that are found in this transition layer are subject to r-b collisions that try to mix the two fluids and are responsible for r-b diffusion. The thickness of the transition layer is, consequently, controlled by the strength and length of long-range potentials and by cross collisions, r-b.

Theoretical difficulty is strongly increased when these two fluids interact with a solid surface. In fact, the interfacial energies ζ^{rs} and ζ^{bs} between fluids r and b and the surface are the main macroscopic mechanisms governing interface advancing or receding on a solid surface. When the interface advances or recedes along a solid surface, dynamic effects will change the contact angle $\theta^{rb/s}$ with respect to its equilibrium value.

Due to the complexity of intermolecular forces and considering their important contribution in defining fluid-fluid and fluid-solid interaction, the lattice Boltzmann method appear to be very suitable as a downscale method that can improve the understanding of complex physical phenomena that are very difficult to describe at the hydrodynamic scale.

In Santos *et al.*, 2003, the field mediators concept, described in dos Santos and Philippi, 2002, was extended for Boltzmann models of immiscible fluids. Mediators are null-mass particles that mimic the action of electrostatic forces. They are emitted from the lattice sites and their only action is to invert the momentum of lattice particles, simulating a long-range field. When a site $\vec{\mathbf{r}}$ can be considered as an attractive center for k particles, $k = r$, b, it will emit mediators of kind k that will be propagated to neighbor sites in the propagation step. Interference of k-mediators pull back to site $\vec{\mathbf{r}}$, k-particles moving away from $\vec{\mathbf{r}}$. In this way, following very simple emission and interference rules, mediators try to simulate the effect of long-range forces in fluid separation. Particles of kind r in the r-b interface that are thrown by collisions toward the b-phase will be pulled back to the r-phase when they found r-mediators in the same site and in the same direction, after propagation step.

Gunstensen *et al.*, 1991, Gunstensen and Rothman, 1992, are attributed to be the first who introduced immiscible fluids color based models in the frame of the lattice Boltzmann method. A more popular two-phase flow model, based on a pseudo-potential function, was derived by Shan and Chen, 1993. This method was later extended to three dimensions, Martys and Chen, 1996. A drawback in the above model is that it become unstable when used to simulate fluids with very different viscositys (say $\mu_1/\mu_2 > 7$), as reported in J. *et al.*, 2002.

In Santos *et al.*, 2003, immiscible fluids r and b are modelled by splitting BGK collision term, separately considering r-r and r-b collisions. In this way, in contrast with the previous models, viscosity coefficients μ_r and μ_b and binary diffusivity $\mathcal{D}_{rb}$ can be independently managed using three independent relaxation times. Interfacial tension is retrieved by modifying r-b collision term, introducing long-range forces in the transition layer through the use of field mediators. Mediators' action is restricted to the transition layer and ideal gas state equation is retrieved for each fluid, far from the interface. In this way, we limit ourselves to an athermal model and no attempt to describe phase transitions and their related effects will be given here.

7.1. A heuristic BGK model for immiscible fluids

In Santos *et al.*, 2003, considering two immiscible fluids r and b, the long-range attraction between the particles of the same species is simulated by producing field mediators on the lattice-sites, just before the propagation step. Considering $R_i(\vec{\mathbf{r}},t)$ to be the particles distribution of r-particles in site $\vec{\mathbf{r}}$ at time t and, similarly, for $B_i(\vec{\mathbf{r}},t)$, mediators are created just before propagation step, and propagated, following

$$M_i^r(\vec{\mathbf{r}}+\vec{\mathbf{e}}_i\delta,t+\delta) = \alpha M_i^r(\vec{\mathbf{r}},t) + \beta\frac{\sum_j R_j(\vec{\mathbf{r}},t)}{\sum_j R_j(\vec{\mathbf{r}},t)+\sum_j B_j(\vec{\mathbf{r}},t)}, \tag{96}$$

where $\alpha+\beta=1$.

The first term in the right hand side of the above equation is, in fact, a recurrence relation, since $M_i^r(\vec{\mathbf{r}},t)$ depends on $M_i^r(\vec{\mathbf{r}}-\vec{\mathbf{e}}_i\delta,t-\delta)$ and on $K_j(\vec{\mathbf{r}}-\vec{\mathbf{e}}_i\delta,t-\delta)$, $K=R,B$, for all j neighbors sites around site $\vec{\mathbf{r}}-\vec{\mathbf{e}}_i\delta$, through second order terms in α and β. In this way, M_i^r at site $\vec{\mathbf{r}}$, will be dependent on the next neighbors r-particles concentration through first order terms, on the second neighbors r-particles through second order terms and so on. When $\alpha=0$ (or $\beta=1$), mediators are created at site $\vec{\mathbf{r}}$, with the solely information of the concentration of r-particles on next neighbors sites: mediators distribution related to the direction i will be given by the mass fraction of r-particles on site $\vec{\mathbf{r}}-\vec{\mathbf{e}}_i\delta$, at time $t-\delta$. In this case, the interaction length corresponds to 1 lattice-unit. By increasing α with respect to β, interaction length can be, arbitrarily, increased.

Mediators are created at each site $\vec{\mathbf{r}}$ and propagated with the unitary lattice velocity $\vec{\mathbf{e}}_i$. The interference of field mediators with lattice-particles is described in the following.

The lattice-Boltzmann equation for kind K particles, is written as

$$K_i(\vec{\mathbf{r}}+\vec{\mathbf{e}}_i\delta,t+\delta)-K_i(\vec{\mathbf{r}},t) = \Omega(R_0,...,R_{b_m},B_0,...,B_{b_m})\ , \tag{97}$$

for $K=R,B$. The collision operator Ω_i^k is required to satisfy the mass and momentum preservation equations,

$$\sum_{i=0}^{b_m}\Omega_i^r = 0\ , \tag{98}$$

$$\sum_{i=0}^{b_m}\Omega_i^b = 0\ , \tag{99}$$

$$\sum_{i=0}^{b_m}\mathbf{c}_i\left(\Omega_i^r+\Omega_i^r\right) = 0\ . \tag{100}$$

A three-parameters BGK collision term that satisfies the above restrictions was proposed in Santos *et al.*, 2003, written as

$$\Omega_i^r = \omega^r\frac{R_i^{eq}(n^r,\vec{\mathbf{u}}^r,T)-R_i}{\tau^r} + \omega^b\frac{R_i^{eq}(n^r,\vec{\mathbf{v}}^{rb},T)-R_i}{\tau^m}\ , \tag{101}$$

where

$$n^k = \sum_{i=0}^{b_m}K_i\ , \tag{102}$$

and

$$\vec{\mathbf{u}}^k = \frac{1}{\rho^k}\sum_{i=1}^{b_m} K_i\vec{\mathbf{c}}_i \ , \tag{103}$$

are, respectively, the macroscopic number density of particles and the velocity of component k, $k = r, b$. The ω's in Eq.101 are the molar fractions, $\omega^k = n^k/n$.

The first term in the r.h.s. of Eq. 101 is related to the relaxation of r-particles distribution to an equilibrium state given by the r-component number density and momentum, considering r-r collisions, only. The second term considers r-b collisions and is related to the relaxation of r-particles to an equilibrium state given by the number density n^r and by the momentum $m^b\vec{\mathbf{u}}^b$modified by the action of r-mediators present in the same site,

$$m^r\vec{\mathbf{v}}^{rb} = m^b\vec{\mathbf{u}}^b - A\vec{\hat{\mathbf{u}}}^m \ , \tag{104}$$

Constant A is to be related to interfacial tension. For ideal miscible fluids, $A = 0$ and this collision term will describe the relaxation of r-particles distribution to an equilibrium state given by n^r and by the momentum $m^b\vec{\mathbf{u}}^b$, as a consequence of r-b cross collisions. In immiscible fluids, Eq. 104 means that particles of kind r will be separated from b-particles by long-range attractive forces from r-phase, represented here by $-\vec{\hat{\mathbf{u}}}^m$.

In the same way,

$$m^b\vec{\mathbf{v}}^{br} = m^r\vec{\mathbf{u}}^r + A\vec{\hat{\mathbf{u}}}^m \ . \tag{105}$$

In Eqs. 104 and 105,

$$\vec{\hat{\mathbf{u}}}^m = \begin{cases} \frac{\vec{\mathbf{u}}^m}{|\vec{\mathbf{u}}^m|} & when\ \vec{\mathbf{u}}^m \neq 0 \\ 0 & when\ \mathbf{u}^m \ = 0 \end{cases} \ , \tag{106}$$

where mediators velocity at site $\vec{\mathbf{x}}$ is given by

$$\vec{\mathbf{u}}^m = \sum_{i=1}^{b_m}(M_i^r - M_i^b)\vec{\mathbf{e}}_i \ , \tag{107}$$

pointing to the same direction where r-mediators were propagated, i.e., to the b-phase.

In present model, since $\left|\vec{\hat{\mathbf{u}}}^m\right| = \{0, 1\}$, the long-range effect on the cross-collision part of Ω_i^r is to relax r-particles distribution to an equlibrium distribution with a $\vec{\mathbf{u}}^0$ velocity, modified, in all lattice sites inside lattice-domains where r and b particles are simultaneously found, by a vector which modulus is constant and equal to A, which is to be related to the net value of interfacial tension. This is not the only choice for satisfying the restrictions on *local* mass and momentum preservation, but the simplest one and, although this could appear as a model 's restriction, the *direction* of $\vec{\hat{\mathbf{u}}}^m$ in a given site $\vec{\mathbf{r}}$ will be dependent on the mediators distribution M_i^r and M_i^b in that site and these distributions are dependent on the r and b particle distributions in the neighbors sites, at the previous time steps.

8. Boundary Conditions

8.1. Monophasic flows inside capillaries

Considering a discrete set of particle velocities $\ell = \{\vec{e}_i, i = 0, ..., b\}$ a boundary condition in the LBM framework can be thought as a reflection law,

$$f_{i^+}(\vec{x}_b^*, t^*) = \sum_j B_{ij} f_{j^-}(\vec{x}_b^*, t^*), \tag{108}$$

where $\vec{e}_{i^+}$ represents a lattice-vector exiting from the solid surface at the site $\vec{x}_b^*$, toward the fluid phase and $\vec{e}_{i^-}$ a lattice vector exiting the fluid phase at the site $\vec{x}_b^*$. The $(b+1)\times(b+1)$ reflection matrix B_{ij} is written in accordance with the macroscopic property it is desired to describe at the boundary.

The simplest and mostly used boundary condition is the bounce-back condition,

$$B_{ij} = \delta_{ij}, \tag{109}$$

giving

$$f_{i^+} = f_{i^-}, \tag{110}$$

which satisfies the adherence condition $\vec{u} = 0$ at the solid boundary.

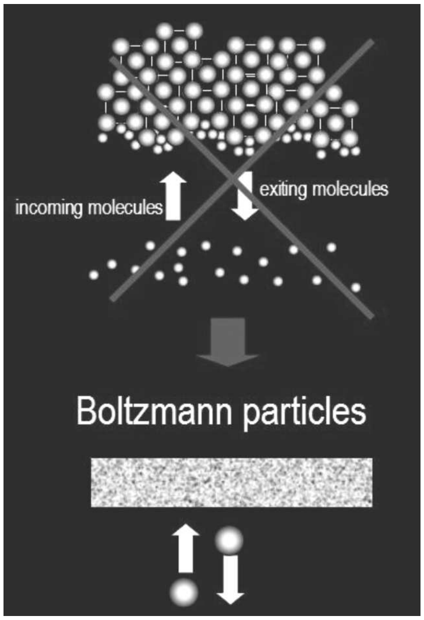

Figure 13: Boundary conditions in LBM.

Bounce-back conditions are pictured in Figure 13. It avoids all the complexity of the description scale related to fluid-solid interaction. At this scale, a certain amount of adsorbed fluid molecules exit the surface, where they, presumably, have reached an equilibrium state with the solid molecules and is replaced by another amount of incoming fluid-molecules from the fluid phase. In steady-state conditions, these incoming and exiting amounts of molecules must be identical. Nevertheless, at this nanometric scale, a slip in the local velocity and a jump in the local temperature are to be expected, since the incoming molecules do not know the equilibrium state that was imposed by the solid surface on the exiting molecules that were adsorbed on it, Philippi and Brun, 1981b. Velocity slips and temperature jumps are dependent on the Knudsen number, i.e., on the ratio between the mean free path and the length of the macroscopic domain of interest. The Knudsen number, itself, is a function of the fluid density and Knudsen discontinuities at the solid surface are only expected to be important, when a low-density gas flows inside a capillary. In this manner, these discontinuities are not expected to be important in liquid-flows. Nevertheless, in the mostly used lattice-BGK collision-propagation schemes, the mean free path is dependent on the dimensionless relaxation parameter τ used for the collision term, since when this parameter grows-up, collisions are less-effective in changing the particles distribution in a given site. In this manner, since the space discretization imposes a numerical lower limit in τ of $1/2$, the Knudsen number is not expected to be small enough, as it is required for a continuum approach, and $\mathcal{O}(Kn^2)$ *numerical* effects are expected to happen in lattice-Boltzmann simulation. These numerical effects are instability sources and these sources are believed to be specially important near the solid walls.

In this way, establishing the correct boundary conditions in LBM is, still, an open problem and a subject of intensive research nowadays.

In athermal problems the bounce-back conditions such as the ones pictured in Figure 13 are in current use and have shown to be suitable for velocity non-slipping problems for several lattices. Adequate boundary conditions for avoiding temperature jumps are still in progress in thermal problems, when a LBE that correctly describes the internal energy balance equation is used.

8.2. Immiscible displacement in capillaries

In immiscible displacement athermal problems, bounce-back conditions are also in use for the particle distributions, but the preferential wettability of one fluid on the solid wall is simulated using different reflection laws for the field mediators (Figure 14). Wettability of a given fluid on a solid surface is related to the relation between the cross adhesion forces among the liquid molecules and the solid and the cohesive forces that happen among the liquid mlecules themselves.

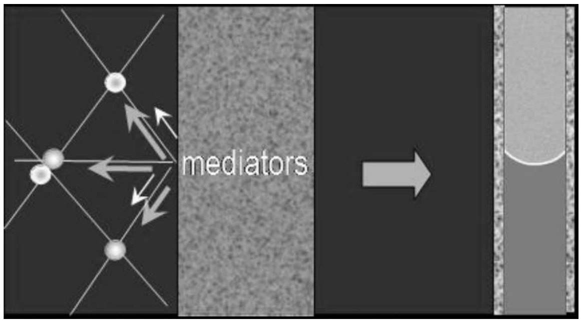

Figure 14: Boundary conditions in immiscible displacement.

The Young's law for liquid drops in contact with a solid surface and with its vapour (or a gas) gives a measurable parameter that quantifies the wettability,

$$\cos\theta_{eq} = \frac{\gamma_{sg} - \gamma_{sl}}{\gamma_l}, \tag{111}$$

where θ_{eq} is the *equilibrium* contact angle, γ_{sg} is the interfacial free energy at the solid-vapour interface reducing to γ_s when the adsorption energy can be neglected, γ_l is the liquid surface tension and, in accordance with Fowkes law,

$$\gamma_{sl} = \gamma_s + \gamma_\ell - \underbrace{\left(2\sqrt{\gamma_s^d\gamma_\ell^d} + 2\sqrt{\gamma_s^p\gamma_\ell^p}\right)}_{\text{adhesion work}}, \tag{112}$$

where the quantity $\left(2\sqrt{\gamma_s^d\gamma_\ell^d} + 2\sqrt{\gamma_s^p\gamma_\ell^p}\right)$ is the adhesion work, W_{ad}.

When $\gamma_{sg} - \gamma_{sl} > \gamma_l$, the adhesive forces are strong and the liquid will spread as a liquid film on the entire solid surface. When $\gamma_{sg} - \gamma_{sl} < \gamma_l$, the cohesive forces among the liquid molecules are dominant.

We have $\gamma_{sg} > \gamma_{sl}$ for a wetting liquid such as water on glass and $\gamma_{sg} < \gamma_{sl}$ for a non-wetting liquid such as mercury. In effect, in accordance with the Fowkes equation above,

$$\gamma_{sg} - \gamma_{sl} = -\gamma_\ell + 2\sqrt{\gamma_s^d\gamma_\ell^d} + 2\sqrt{\gamma_s^p\gamma_\ell^p}, \tag{113}$$

and this quantity can be either positive, when $\gamma_\ell < 2\sqrt{\gamma_s^d\gamma_\ell^d} + 2\sqrt{\gamma_s^p\gamma_\ell^p}$, i.e., when the liquid surface tension is smaller than the mixing cross forces among the liquid molecules and the solid surface, or negative, when the liquid surface tension (related to the intermolecular forces among the liquid molecules themselves) are stronger than the forces among liquid and solid molecules.

Oil and water are both wetting fluids on, e.g., a glass surface. Nevertheless, for water, w, the cross mixing forces with the glass molecules are strong giving a large adhesion work and a small γ_{sw}, when compared with an oil, o, such as isopentano, with a small adhesion work and a large γ_{so}. When water and oil are in contact with a solid surface

$$\cos\theta_{eq} = \frac{\gamma_{so} - \gamma_{sw}}{\gamma_{rb}}. \tag{114}$$

Present lattice-Boltzmann schemes for simulating immiscible displacement in capillaries are based on rather simple rules, by adjusting the reflected amounts of fluids r and b in such a maner as to retrieve the equilibrium contact angle in equilibrium simulations (Figure 15). In this way, in addition to the viscosity ratio, the only experimental information that is needed in these kind of simulations are the equilibrium contact angle, θ_{eq} and the interfacial tension, γ_{rb}. Further studies are necessary for including the polar and dispersive surface energies in the model parameters.

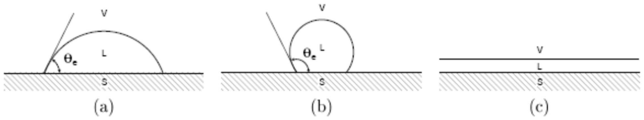

Figure 15: Equilibrium between a liquid drop and a solid surface for (a) a wetting liquid, (b) a non-wetting liquid and (c) a totally spreading liquid.

9. A sample problem: capillary invasion

The simulation results of the capillary invasion of a wetting liquid, r, into a cylindric tube, under zero gravity, is shown in Figure 16. Only capillary forces are considered and, in this way, the pressure in the capillary entrance and exit were kept the same, the non-wetting fluid particles, b, that exit the numerical domain being reintroduced at the capillary entrance, after they change their label as wetting fluid r-particles. A model similar to the one that was developed for immiscible fluids was used. The fluid viscosities and the interfacial tension are the only informations required for the model, when the fluid-solid interaction is not considered.

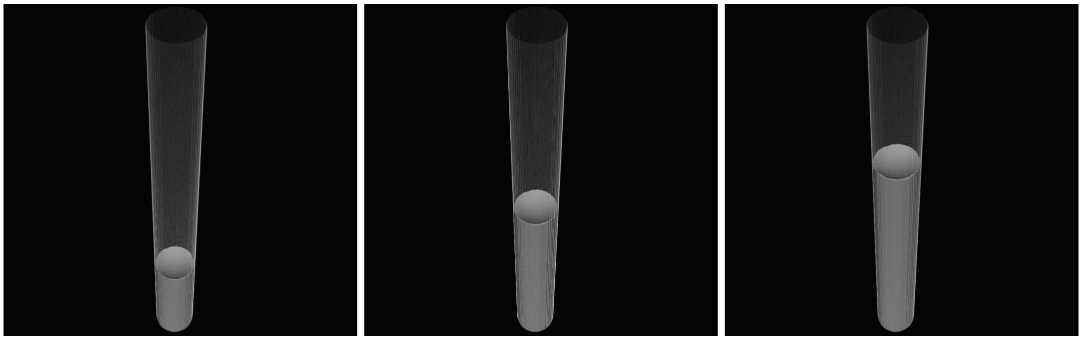

Figure 16: Capillary invasion

The LBM simulation was performed without any velocity singularity in the triple line, since the triple-line is here considered as a *transition region* where the fluid-particles are subjected to electrostatic forces from the wall and from the fluid phases.

In the fluid-fluid interface the electrostatic attractive forces among, e.g., the r-particles and the r-phase are simulated by deviating a certain amount of r-particles to the r-phase in accordance with Eq. (101), in the direction from where the r-mediators were emitted (Figure 16). This amount, which is the same for b-particles, is given by the force parameter A, in Eq. (104), directly related to the γ_{rb} interfacial tension (Santos *et al.*, 2003).

Boundary conditions are reflection laws for the particles and the mediators such as the ones described in the above section. The reflected amounts of r and b mediators are kept constant and adjusted in accordance with a given equilibrium contact angle, θ_{eq} in static conditions.

In this manner, in capillary invasion, the wetting fluid r-particles in the triple line will be simultaneously subjected to the attraction forces from the r-phase and from the solid surface, since the incoming mediators, after reflection on the solid wall, are predominantely r-mediators. From Figure 17, it can be seen that the predominancy of the fluid adhesion to the solid surface with respect to the cohesive forces to the r-phase, will be decided by the larger relative value of the horizontal projection of the attractive force from the wall, with respect to the atractive force from the r-phase.

A Poiseuille parabolic velocity profile was obtained in both phases for points that are far enough from the interface and from the tube entrance. Figure 18 shows the streamlines near the fluid-fluid interface in the

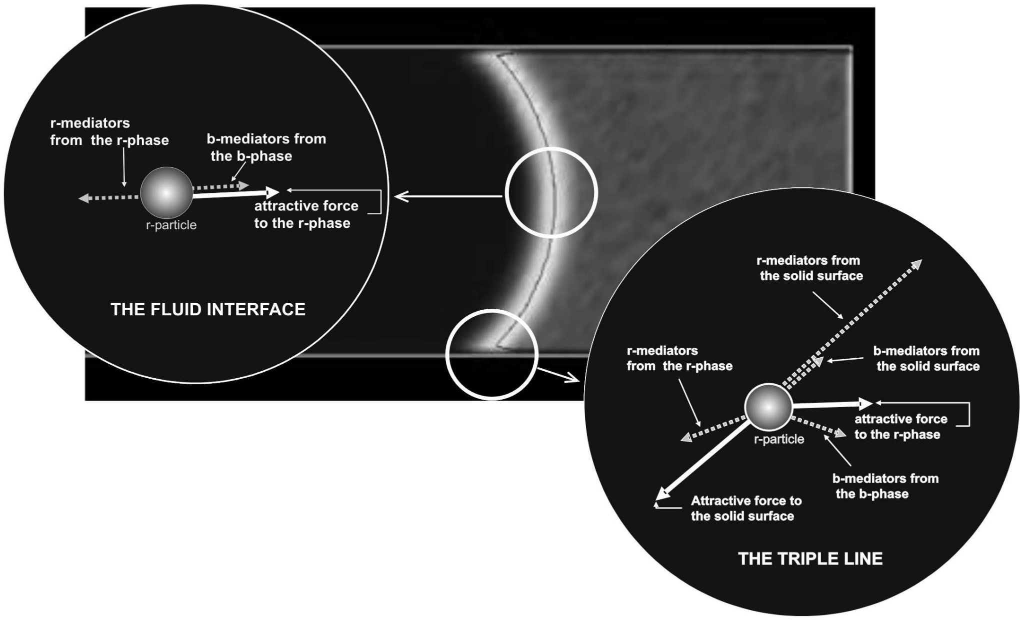

Figure 17: The fluid-fluid interface and the triple line.

course of the capillary invasion, at a symmetry plane. A strong recirculating zone, a vortex, is presented near the triple line. The vortex length is dependent on the strength and on the interaction length of the fluid-fluid and fluid-solid electrostatic forces. It belongs, indeed, to the same nanometric scale that is used for describing the triple-line itself and cannot be accessed by experimental visualizations.

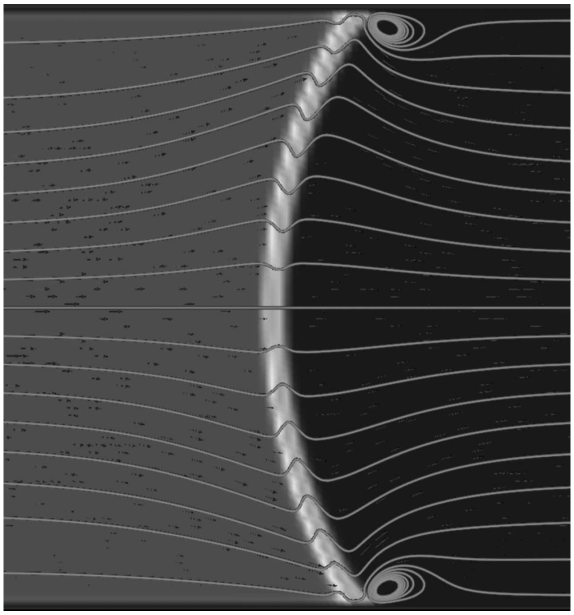

Figure 18: Streamlines near the fluid-fluid interface, showing a recirculating flow close to the triple-line.

In this way, the physical structure of this vortex is dependent on the model that was used for describing the capillary invasion process and this model cannot be validated against experimental results, at this nanometric scale. Nevertheless, Figure 19, a macroscopic result from the present LBM simulations, shows the capillary number dependence of the dynamic contact angle, as

$$\cos \theta_d = \cos \theta_e - \alpha Ca^{\beta} \tag{115}$$

where the capillary number is

$$Ca = \frac{\mu_r}{\gamma_{rb}} u_{int} \tag{116}$$

and u_{int} is the interface velocity. Angle θ_e is the equilibrium contact angle at static conditions. Eq. (115) was verified to be in correct agreement with experimental visualizations.

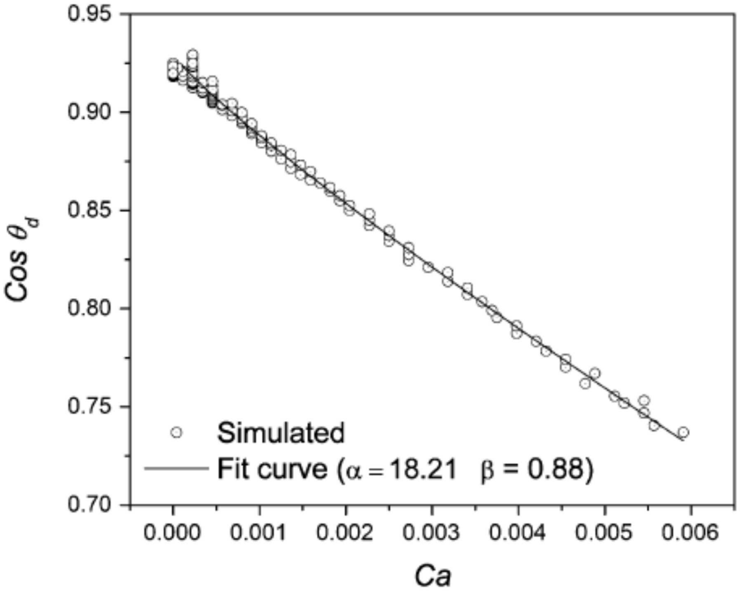

Figure 19: Capillary number dependence of the dynamical contact angle.

10. Conclusion

In spite of its great technological importance and of the growing scientific interest, microhydrodynamics has still a number of open questions to solve since macroscopic methods based on the Navier-Stokes framework have revealed to be insufficient to solve dynamic problems when interfacial forces and surface phenomena play an important role in the description of the problem. Although the great development of up-scaling methods from the molecular to the macroscopic scales based on the Boltzmann mesoscopic equation: a) the Boltzmann equation itself appropriated for liquids, taking the finite volume of particles and long range interaction into account, is still under investigation; b) The discretization of the Boltzmann equation leading to a manageable numerical method has not a unique issue when the computer limitations must be considered.

In this work, these several questions were discussed and some main problems in constructing a numerical method based on the spatial and velocity discretization of the Boltzmann equation were presented.

11. References

Alexander, F. J., Chen, S., and Sterling, J. D., 1993, Lattice Boltzmann Thermohydrodynamics, “Phys. Rev. E”, Vol. 47, No. 4, pp. R2249.

Amyot, O., 2004, “Contribution à l’ étude des é coulements diphasiques à travers un contact rugueux”, PhD thesis, University of Poitiers.

Bhatnagar, P., Gross, E., and Krook, M., 1954, A Model for Collision Processes in Gases. I. Small Amplitude Processes in Charged and Neutral One-Component Systems, “Phys. Rev.”, Vol. 94, pp. 511.

Boltzmann, L., 1866, Über die Mechanische Bedeutung des Zweiten Hauptsatzes der Wärmetheorie, “Wiener Berichte”, Vol. 53, pp. 195–220.

Bosanquet, C., 1923, “Phils. Mag. ser.”, Vol. 6.

Bretherton, F. P., 1961, The Motion Of Long Bubbles In Tubes, “Journal Of Fluid Mechanics”, Vol. 10, pp. 166–188.

Cercignani, C., 1969, “Mathematical Methods in Kinetic Theory”, Macmillan, London, first edition.

Chapman, S. and Cowling, T., 1999, "The Mathematical Theory of Non-Uniform Gases", Cambridge University Press, Cambridge.

Chen, H., Chen, S., and Matthaeus, W. H., 1992, Recovery of the Navier-Stokes equations using a lattice-gas Boltzmann method, "Phys. Rev. A", Vol. 45, No. 8, pp. R5339.

Chen, S., Chen, H., Martinez, D., and Matthaeus, W. H., 1991, Lattice Boltzmann model for simulation of magnetohydrodynamics, "Phys. Rev. Lett.", Vol. 67, pp. 3776.

Chen, Y., Ohashi, H., and Akiyama, M., 1994, Thermal Lattice Bhatnagar-Gross-Krook Model Without Non-linear Deviations In Macrodynamic Equations, "Phys. Rev. E", Vol. 50, No. 4, pp. 2776.

d'Humières, D., 1992, Generalized lattice-Boltzmann equation, Shizgal, B. D. and Weaver, D. P., editors, "Progress in Astronautics and Aeronautics", Vol. 159, pp. 450–458.

d'Humières, D., Bouzidi, M., and Lallemand, P., 2001, Thirteen-velocity three-dimensional lattice Boltzmann model, "Phys. Rev. E", Vol. 63, No. 6, pp. 066702.

dos Santos, L. and Philippi, P. C., 2002, Lattice-gas model based on field mediators for immiscible fluids, "Phys. Rev. E", Vol. 65, pp. 046305.

Dussan, E. B., Ramé, V. E., and Garoff, S., 1991, On Identifying The Appropriate Boundary-Conditions At A Moving Contact Line - An Experimental Investigation, "Journal Of Fluid Mechanics", Vol. 230, pp. 97–116.

Enskog, D., 1921, Kinetiske theorie, "Svenska Vet. Akad. Handl.", Vol. 63, No. 4.

Fowkes, F., 1972, Donor-Acceptor Interactions At Interfaces, "Journal Of Adhesion", Vol. 4, No. 2, pp. 155.

Gunstensen, A. and Rothman, D., 1992, Microscopic Modeling Of Immiscible Fluids In 3 Dimensions By A Lattice Boltzmann Method, "Europhysics Letters", Vol. 18, pp. 157–161.

Gunstensen, A., Rothman, D., Zaleski, S., and Zanetti, G., 1991, Lattice Boltzmann Model Of Immiscible Fluids, "Physical Review A", Vol. 43, pp. 4320–4327.

He, X., Chen, S., and Doolen, G. D., 1998, A novel thermal model for the lattice Boltzmann method in incompressible limit, "J. Comput. Phys.", Vol. 146, No. 1, pp. 282–300.

He, X. and Doolen, G. D., 2002, Thermodynamic foundations of kinetic theory and Lattice Boltzmann models for multiphase flows, "J. Stat. Phys.", Vol. 107, No. 1–2, pp. 309–328.

He, X. and Luo, L. S., 1997, Theory of the lattice Boltzmann method: From the Boltzmann equation to the lattice Boltzmann equation, "Phys. Rev. E", Vol. 56, No. 6, pp. 6811–6817.

Higuera, F. J. and Jimenez, J., 1989, Boltzmann Approach To Lattice Gas Simulations, "Europhys. Lett.", Vol. 9, pp. 663.

Israelachvili, J. N., 1992, "Intermolecular and surface forces", Academic Press.

J., C., .S., B. E., and V., C. P., 2002, Lattice Boltzmann simulation of the flow of binary immiscible fluids with different viscosities using the Shan-Chen microscopic interaction model, "Philosophical Transactions Of The Royal Society Of London Series A-Mathematical Physical And Engineering Sciences", Vol. 360, pp. 547–558.

Kremer, G. M., 2005, "Uma Introdução à Equação de Boltzmann", Editora da Universidade de São Paulo.

Lallemand, P. and Luo, L. S., 2003, Theory of the lattice Boltzmann method: Acoustic and thermal properties in two and three dimensions, "Phys. Rev. E", Vol. 68, No. 3, pp. 036706.

Landau, L. D. and Levich, V. G., 1942, Dragging of a liquid by a moving plate, "Acta Phys. Chim. Urss", Vol. 17, pp. 42–54.

Lifshitz, E. and Pitaevskii, L., 1999, "Phyical kinetics", Butterworth-Heinemann, Oxford.

Lucas, R., 1918, Ueber das Zeitgesetz des Kapillaren Aufstiegs von Flussigkeiten, "Kolloid Z.", Vol. 23, No. 15.

Martys, N. S. and Chen, H., 1996, Simulation of multicomponent fluids in complex three-dimensional geometries by the lattice Boltzmann method, "Phys. Rev. E", Vol. 53, pp. 743–750.

McNamara, G. and Alder, B. J., 1993, Analysis Of The Lattice Boltzmann Treatment Of Hydrodynamics, "Physica A", Vol. 194, No. 1–4, pp. 218–228.

McNamara, G. R. and Zanetti, G., 1988, Use of the Boltzmann Equation to Simulate Lattice-Gas Automata, "Phys. Rev. Lett.", Vol. 61, No. 20, pp. 2332.

Ortiz, C. E. P., dos Santos, L., and Philippi, P., 2006, A two-fluid lattice Boltzmann model for ideal mixtures, "15^{th} DSFD - Discrete Simulation of Fluid Dynamics", Geneve.

Philippi, P.C.and Hegele Jr, L. A., Surmas, R., Siebert, D., and dos Santos, L., 2006a, From the continuous to the lattice-Boltzmann equation: beyond BGK collision models, "15^{th} DSFD - Discrete Simulation of Fluid Dynamics", Geneve.

Philippi, P., Hegele Jr., L., and dos Santos, L.O.E. andSurmas, R., 2006b, From the continuous to the lattice Boltzmann equation: The discretization problem and thermal models, "Phys. Rev. E", Vol. 73, No. 5, pp. 056702.

Philippi, P., Hegele Jr, L. A., Surmas, R., Siebert, D., and dos Santos, L. E., 2006c, Thernal lattice-Boltzmann in two dimensions, "15^{th} DSFD - Discrete Simulation of Fluid Dynamics", Geneve.

Philippi, P. C. and Brun, R., 1981a, Kinetic Modeling Of Polyatomic-Gas Mixtures, "Physica A", Vol. 105, No. 1-2, pp. 147–168.

Philippi, P. C. and Brun, R., 1981b, Kinetic Models and Relaxation Effects in the Knudsen Layer of Gas Mixtures, “Progress in Astronautics and Aeronautics”, Vol. 74, pp. 428–443.

Qian, Y. H., d’Humières, D., and Lallemand, P., 1992, Lattice Bgk Models For Navier-Stokes Equation, “Europhys. Lett.”, Vol. 17, No. 6, pp. 479.

Santos, L. O. E., Facin, P. C., and Philippi, P. C., 2003, Lattice-Boltzmann model based on field mediators for immiscible fluids, “Physical Review E”, Vol. 68, No. 5, pp. 056302.

Shan, X. and Chen, H., 1993, Lattice Boltzmann Model For Simulating Flows With Multiple Phases And Components, “Phys. Rev. E”, Vol. 47, pp. 1815–1819.

Shan, X. and He, X., 1998, Discretization of the velocity space in the solution of the Boltzmann equation, “Phys. Rev. Lett.”, Vol. 80, No. 1, pp. 65–68.

Shan, X., Yuan, X. F., and Chen, H., 2006, Kinetic theory representation of hydrodynamics: a way beyond the Navier-Stokes equation, “Journal Of Fluid Mechanics”, Vol. 550, pp. 413–441.

Stange, M., Dreyer, M. E., and Rath, H. J., 2003, Capillary driven flow in circular cylindrical tubes, “Physics of Fluids”, Vol. 15, No. 9, pp. 2587–2601.

Surmas, R., 2006, Desenvolvimento de um modelo de Boltzmann para redes adequado a análise de problemas não-isotérmicos envolvendo fluidos não-ideais com transição de fases, Technical report, Mechanical Engineering Graduate Program Federal University of Santa Catarina.

Surmas, R., Ortiz, C. P., and dos Santos, L.O. E.and Philippi, P., 2006, Volume exclusion for reducing compressibility effects in lattice-Boltzmann models, “15^{th} DSFD - Discrete Simulation of Fluid Dynamics”, Geneva.

Tanenbaum, B., 1987, “Plasma Physics”, McGraw Hill, New York.

Wang Chang, C. and Uhlenbeck, G., 1970, “Sudies of Statistical Mechanics”, Vol. 5. North-Holand, Amsterdam.

Washburn, E. W., 1921, The Dynamics of Capillary Flow, “Physical Review”, Vol. 17, No. 3, pp. 273.